ANNUAL REVIEWS

Annual Review of Biomedical Engineering

Structural DNA Nanotechnology: Artificial Nanostructures for Biomedical Research

Yonggang Ke,[1] Carlos Castro,[2] and Jong Hyun Choi[3]

[1]Wallace H. Coulter Department of Biomedical Engineering, Georgia Institute of Technology and Emory University, Emory University School of Medicine, Atlanta, Georgia 30322, USA; email: yonggang.ke@emory.edu

[2]Department of Mechanical and Aerospace Engineering, The Ohio State University, Columbus, Ohio 43214, USA

[3]School of Mechanical Engineering, Purdue University, West Lafayette, Indiana 47907, USA

Annu. Rev. Biomed. Eng. 2018. 20:375–401

First published as a Review in Advance on April 4, 2018

The *Annual Review of Biomedical Engineering* is online at bioeng.annualreviews.org

https://doi.org/10.1146/annurev-bioeng-062117-120904

Keywords

DNA, static nanostructures, dynamic nanostructures, biosensing, bioimaging, drug delivery

Abstract

Structural DNA nanotechnology utilizes synthetic or biologic DNA as designer molecules for the self-assembly of artificial nanostructures. The field is founded upon the specific interactions between DNA molecules, known as Watson–Crick base pairing. After decades of active pursuit, DNA has demonstrated unprecedented versatility in constructing artificial nanostructures with significant complexity and programmability. The nanostructures could be either static, with well-controlled physicochemical properties, or dynamic, with the ability to reconfigure upon external stimuli. Researchers have devoted considerable effort to exploring the usability of DNA nanostructures in biomedical research. We review the basic design methods for fabricating both static and dynamic DNA nanostructures, along with their biomedical applications in fields such as biosensing, bioimaging, and drug delivery.

Contents

1. INTRODUCTION

DNA (deoxyribonucleic acid) is the genetic information carrier for all known living organisms and some viruses. It is a biopolymer of nucleotides, with each nucleotide containing one of four nucleobases, cytosine (C), guanine (G), adenine (A), or thymine (T); a deoxyribose; and a phosphate group. The interaction between two DNA biopolymers or strands is determined by the coding of bases, known as Watson–Crick base pairing (1), where A pairs with T and C pairs with G through hydrogen bonding. Massive amounts of information, genetic or nongenetic (2), can be stored in a long piece of DNA with defined sequences.

From a material perspective, the unique characteristics of DNA make it a promising and versatile material candidate for a wide range of applications. For instance, the DNA double helix (e.g., B-form) has a diameter of 2 nm and a helical turn of 10.5 bp (or 3.4 nm). More importantly, the interactions between DNA molecules are specifically governed by Watson–Crick base pairing. Such specificity has led to the programmability of DNA interactions and the foundation of structural DNA nanotechnology. Structural DNA nanotechnology is the field in which DNA (or RNA) molecules are utilized as building blocks for self-assembly into artificial nanostructures. Its conceptual foundation can be traced to 1982, when Seeman (3) proposed utilizing DNA structures to aid the crystallization of proteins. Three decades of development have led to the use of DNA as a designer molecule with an enormous capacity to construct both static and dynamic nanostructures with unprecedented precision and complexity. These DNA nanostructures are a set of materials with unique properties (e.g., well-defined size, geometry, interactions) that can be utilized on their own or be combined with other materials for many biomedical applications. For example, pristine DNA nanostructures have been used to interact with biological systems to enable biosensing (4), bioimaging (5), or drug delivery (6). In this review, we describe the basic design principles and representative examples of both static and dynamic DNA nanostructures. We also present a comprehensive review of the biomedical applications of such DNA nanostructures.

2. DNA NANOSTRUCTURES

Self-assembled DNA nanostructures are categorized into static and dynamic nanostructures. There are two basic design strategies to construct DNA nanostructures: the DNA tile technique and the later-developed DNA origami approach. Both strategies are founded upon the unique programmability of DNA base pairing.

2.1. Static DNA Nanostructures

DNA tiles are a set of artificial structures composed of several DNA single strands with unique sequences, whose hierarchical assembly leads to the formation of large DNA structures. Seeman et al. (7) reported the first DNA tile, named the immobile four-way junction, that was built from four single DNA strands (**Figure 1*a***). This DNA tile closely resembles the natural Holliday junction, in which strand migration is prevented by minimizing the sequence symmetry in the junction. Three-, five-, six-, eight-, and 12-way junctions have been constructed via the same strategy (8–10). Nevertheless, such DNA tiles failed to assemble into higher-order structures due to significant structural flexibility both on and off the tile plane. Rigid DNA double-crossover (DX) structures were then proposed and fabricated (11). In these structures, two four-way junctions are confined within two parallel DNA double helices by two crossovers (**Figure 1*b***). In 1998, a two-dimensional (2D) DNA crystal structure was fabricated through sticky-end mediated assembly of a two-arm DX tile (**Figure 1*c*, *i***) (12). This was the first example of a higher-order crystal-like structure assembled from DNA, representing a milestone in the field of structural DNA nanotechnology.

Subsequently, DNA 2D crystals containing diverse and complex patterns were assembled from three-arm (14), four-arm (13, 27), five-arm (17), or six-arm (15) DNA tiles (**Figure 1*c*, *ii–v***). Combining the assembly of multiple DNA tile designs with a variable number of arms resulted in 2D crystals of much higher complexity, such as Archimedean crystals (28, 29). The field has long pursued three-dimensional (3D) DNA crystals, beginning with a DNA tensegrity triangle tile created in 2009 (**Figure 1*c*, *vi***) (18). In addition to infinite-size crystal structures, 3D polyhedral structures (**Figure 1*d***) can be constructed from DNA tiles (16, 17, 21, 23–26). These DNA tile designs typically produce highly periodic and symmetric structures and thus are unable to construct arbitrary structures with well-defined size, shape, and pattern. In a complement to conventional DNA tile designs, Yin and colleagues (19, 20) developed a special type of DNA tile referred to as a single-stranded DNA (ssDNA) tile (SST), later referred to as a DNA brick. In DNA brick design, each ssDNA has a unique sequence and acts as a molecular brick to intact with other bricks, forming the designed 2D (**Figure 1*e*, *i***) (20) or 3D (**Figure 1*e*, *ii***) (19) object. A unique advantage of DNA brick design is its modularity. In other words, a master set of DNA strands can serve as a 2D or 3D canvas, enabling the construction of a large number of arbitrary DNA objects simply by excluding designated strands. This method enables one to build a library of DNA objects with arbitrary sizes and shapes in a high-throughput fashion. Similar to conventional DNA tiles, DNA bricks can be induced to form infinite-size crystal structures by bridging the head and tail bricks (**Figure 1*e*, *iii***) (22).

Origami refers to the art of folding and sculpting flat paper into objects with arbitrary shapes. DNA origami, reported by Rothemund (30) in 2006, creates similar art at the nanoscale. In the molecular self-folding process, a long ssDNA (scaffold DNA), typically the M13 bacteriophage genome DNA (~7,000 nt), is folded into designed objects with well-defined geometry by hundreds of synthetic, short (20–60 nt) ssDNAs (known as staple DNAs). Note that, prior to the DNA origami era, a few studies demonstrated similar concepts. For instance, in 2003, Yan et al. (31) ligated ssDNAs into longer molecules to serve as scaffolds to direct the nucleation of DNA tiles forming discrete objects or lattice structures with bar-code patterns (**Figure 2*a*, *i–ii***). A year later, Shih et al. (32) folded a 1,669-nt-long ssDNA molecule into a 3D octahedron with five 40-nt-long synthetic DNA molecules (**Figure 2*a*, *iii–iv***). Nonetheless, these two studies did not demonstrate the versatility of this technique for the construction of DNA objects with complex and arbitrary geometries.

The use of commercially available ssDNA (M13 DNA) as a scaffold is another unique benefit introduced by Rothemund. Two distinct DNA origami design strategies have been developed so far: lattice-based origami and wire-frame origami (**Figure 2*b–d***). These methods differ in the

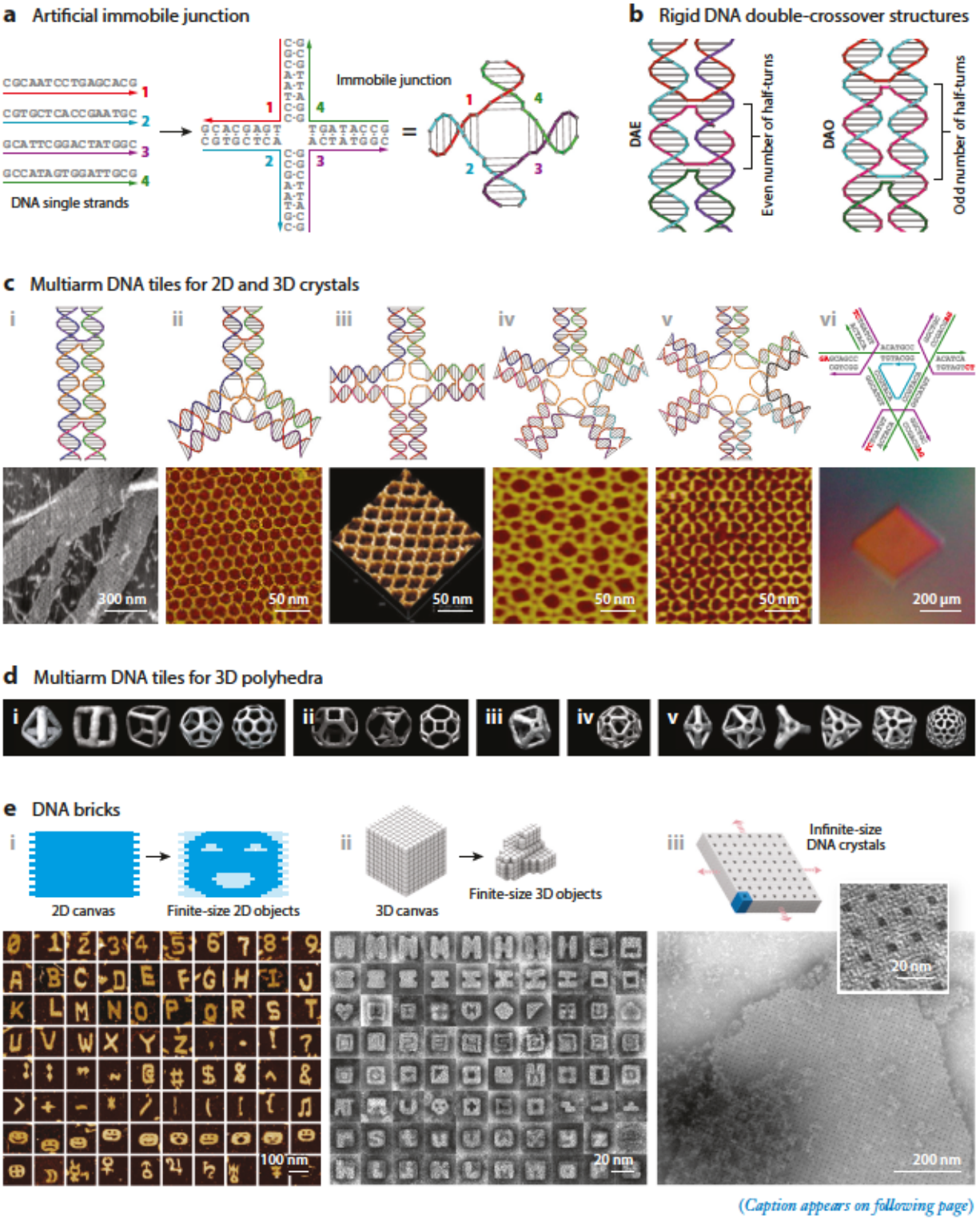

(Caption appears on following page)

Figure 1 *(Figure appears on preceding page)*

Static nanostructures assembled from DNA tiles. (*a*) Artificial immobile junction assembled from four DNA strands. (*b*) Rigid double-crossover structures. (*c*) Multiarm DNA tiles for two-dimensional (2D) and three-dimensional (3D) crystals. (*i–v*) 2D crystals assembled from DNA tiles with (*i*) two, (*ii*) three, (*iii*) four, (*iv*) five, and (*v*) six arms. (*vi*) 3D crystals assembled from a DNA tensegrity triangle tile. (*d*) Polyhedral structures assembled from (*i*) a symmetric three-arm tile, (*ii*) an asymmetric three-arm tile, (*iii*) a four-arm tile, (*iv*) a five-arm tile, and (*v*) hybrid tiles. (*e*) DNA bricks for the assembly of (*i*) finite-size 2D objects, (*ii*) 3D objects, and (*iii*) infinite-size DNA crystals. Abbreviations: DAE, DNA antiparallel double-crossover separated by an even number of half-turns; DAO, DNA antiparallel double-crossover separated by an odd number of half-turns. Modified with permission from References 7 and 11–26.

arrangement of helices within the DNA origami objects. Earlier DNA origami studies built upon the lattice-like packing of DNA helices, in which the helices were closely packed into square (30, 33), honeycomb (34), hexagonal (35), or hybrid lattices (35). Flat 2D objects, such as the famous smiley face (**Figure 2*c*, *i***), were the first to be constructed (30). Further folding of flat 2D origami sheets led to the formation of hollow 3D containers, such as a DNA box (**Figure 2*c*, *ii***) (36) and a tetrahedron (37). In contrast to the folding of 2D flat sheets, the interhelical angles and length of adjacent DNA helices were arranged into concentric rings that can be rationally designed to induce curvature in 3D space and thus form hollow 3D objects with complex shapes (**Figure 2*c*, *iii***) (38). Solid 3D DNA origami objects can be assembled via close-packing DNA helices into lattices in 3D space (**Figure 2*c*, *iv***) (33–35). Curvature can be introduced into solid objects via rationally adding or deleting bases between crossovers (39).

In contrast to lattice-based DNA origami, wire-frame DNA origami produces porous structures by minimizing the packing of DNA helices. For instance, Yan and colleagues (40) used DNA four-arm junctions as vertices of a DNA network to fabricate DNA gridiron structures (**Figure 2*d*, *i***). Multiarm junctions (49) were then used to construct wire-frame DNA origami structures with greater complexity (**Figure 2*d*, *ii***). Bathe and colleagues (51) developed an algorithm named DAEDALUS that enabled the automated design of a large library of polyhedral structures (**Figure 2*d*, *iii***). Högberg and colleagues (47) reported an alternative wire-frame strategy that renders designed objects into meshes. 3D objects, such as the Stanford bunny (**Figure 2*d*, *iv***), have been fabricated through this method. Wire-frame DNA origami excels at constructing arbitrary-shaped, soft, and porous structures. The loose arrangement of the DNA helices means that wire-frame DNA origami structures have high resistance against cation (e.g., Mg^{2+}, Na^{+}) depletion, as cations are needed to shield the natural negative charge of DNA helices in order to realize close packing (47, 51). Therefore, wire-frame structures have greater potential for intracellular applications because physiological fluids have a relatively low abundance of cations.

Both scaffold and staple DNA can be engineered to build larger DNA origami structures. Fan and colleagues (44) utilized polymerase chain reaction to produce a 26,182-nt-long scaffold DNA molecule (**Figure 2*e*, *i***). LaBean and colleagues (46) constructed a M13-λ hybrid phage to produce a 51,466-nt-long scaffold DNA molecule that yielded origami structures that were seven times as massive as ordinary M13-based structures (**Figure 2*e*, *ii***). Structures preassembled from DNA tiles (41) or DNA origami (43) can serve as superstaples to fold the M13 scaffold into much larger structures (**Figure 2*e*, *iii–iv***). An alternative route is the hierarchical assembly of DNA origami tiles, which can be realized through sticky-end cohesion or blunt-end stacking. For instance, symmetric polyhedral structures have been assembled from DNA origami tripod (**Figure 2*f*, *i***) (45); a nanoman was assembled from many units of a DNA origami square (**Figure 2*f*, *ii***) (50). Micrometer-scale DNA origami lattices containing hundreds of DNA origami tiles can also be created (**Figure 2*f*, *iii–iv***), either in solution (42, 48, 52) or on a substrate (53–56).

Many software programs and algorithms exist to facilitate the design of complex DNA structures. For instance, Tiamat is employed for the design of DNA tiles and simple DNA origami

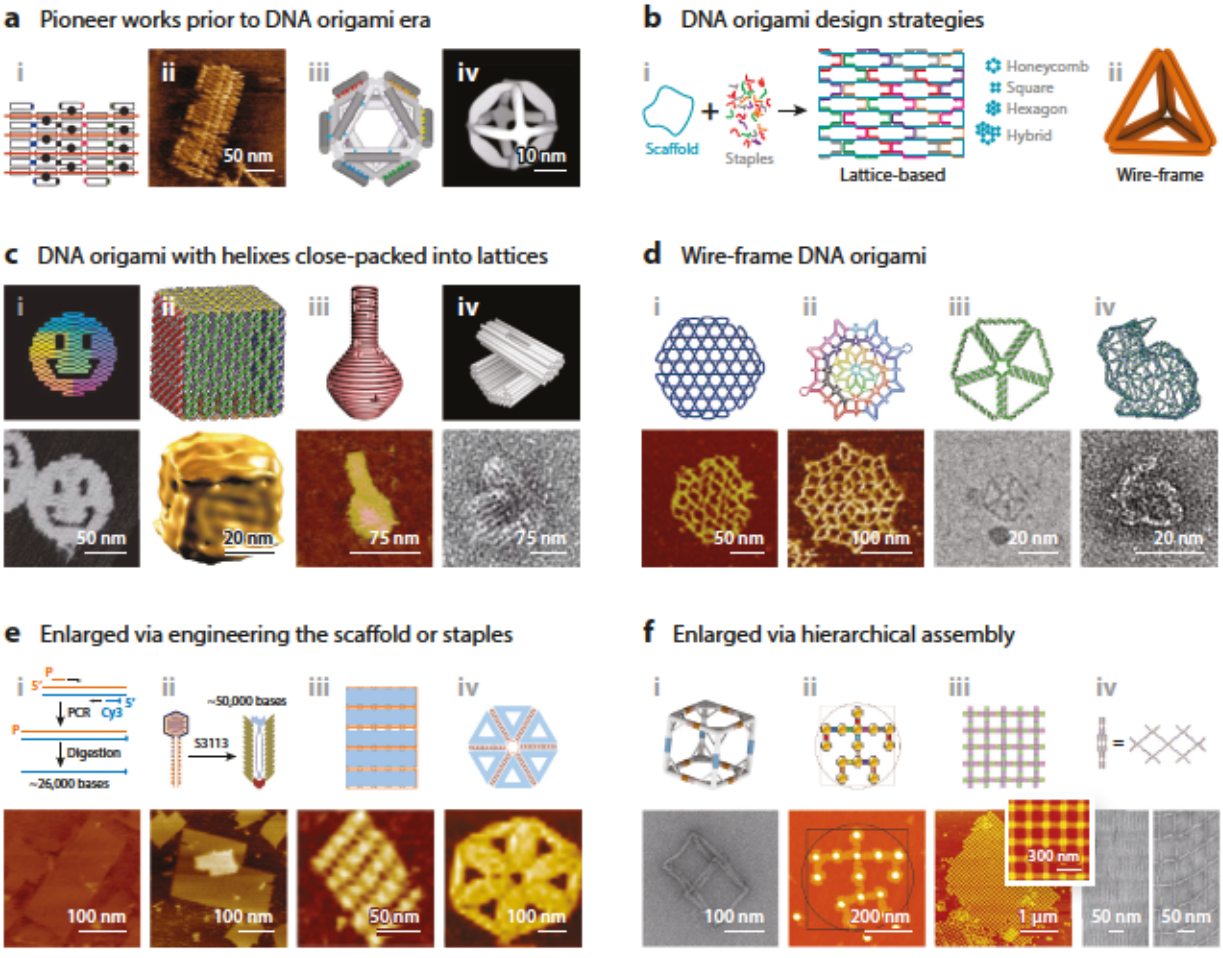

Figure 2

Static nanostructures assembled from DNA origami. (*a*) Early concepts created prior to the birth of DNA origami. (*b*) Two basic DNA origami design strategies: lattice-based versus wire-frame origami. (*c*) Representative two-dimensional (2D) and three-dimensional (3D) objects assembled from lattice-based DNA origami. (*d*) Representative 2D and 3D objects assembled from wire-frame DNA origami. (*e*) DNA origami enlarged via engineering of the scaffold or the staples. (*f*) DNA origami enlarged via the hierarchical assembly of building blocks mediated by sticky-end cohesion or blunt-end stacking. Abbreviations: Cy3, cyanine 3; PCR, polymerase chain reaction; P, phosphorylated primer. Modified with permission from References 30–32, 34, 36, 38, and 40–51.

structures. NanoBricks is used for the design of DNA brick structures. caDNAno (57) excels at designing lattice-based DNA origami structures. DAEDALUS (51) works within MATLAB and Python to design wire-frame DNA origami structures. Detailed information about the design process can be found in the references provided.

2.2. Dynamic DNA Nanostructures

The ability to design precise complex geometry at the molecular scale renders structural DNA nanotechnology capable of constructing nanomaterials, devices, and machinery that can sense, respond to, and navigate the local environment; transfer motion, forces, and energy; and process

and communicate information. Constructing dynamic DNA-based devices with these functions generally requires integrating various underlying components with a range of mechanical and chemical properties, including flexibility and biochemical addressability. In general, several types of dynamic features, such as constrained thermal fluctuation for diffusive search processes, programmed machine-like planar (2D) or spatial (3D) motion, precise conformational changes, and tunable distribution of states, can be designed into devices by use of mechanical design features.

The components for mechanical design can be broken down into combinations of flexible elements (e.g., ssDNAs), compliant or deformable elements [double-stranded DNAs (dsDNAs) or bundles of only a few dsDNAs], and stiff elements (e.g., bundles of dsDNAs with many helices in the cross section) (58). At length scales shorter than 50 nm, the persistence length of dsDNA (59, 60), individual dsDNA helices can also function as stiff components. Typically, local motions are facilitated by the flexible elements, or deformation can be distributed over compliant elements. These local or distributed motions can be translated into larger motions or conformational changes by stiff elements. Integrating these components enables the design of dynamic DNA nanodevices with a range of functions. In general, dynamic DNA nanodevices can be classified into DNA motors (walkers and rollers), reconfigurable strand systems, systems with local reconfiguration of strands or subunits within larger templates, triggered containers, mechanical joints, and multijoint mechanisms (**Figure 3**).

DNA motors, recently reviewed by Pan et al. (61), undergo processive motion by moving along successive binding sites organized along a track. Binding to the track is achieved by base-pairing interactions between ssDNAs on the device and complementary ssDNAs on the track. To achieve processive motion, the device must remain bound to the track by at least one binding site during successive steps. DNA walkers often contain two track-binding ssDNAs (62–67) so that one can remain anchored while the other steps to a neighboring binding site via a diffusive search between the two complementary strands. Once both strands are anchored to the track, the motion proceeds by biasing a step toward the leading strand that occurs via mechanisms to release the lagging binding site, such as strand displacement (62–67). Alternatively, walking can be driven enzymatically through the use of enzymes that nick the track strand when it is hybridized to the walker strand (68, 69). The track strand leaves a toehold region so that a neighboring track strand can displace the prior anchoring site. This approach is referred to as the burned-bridges approach because the walker can proceed only in the direction of undigested track strands. Rollers proceed along tracks via similar mechanisms, but engagement of successive binding sites along the track occurs through the rolling motion of a rigid particle (71, 72, 90).

Track substrates include DNA (62–65, 67, 69, 71, 90–92), carbon nanotubes (70, 93), glass or gold-coated surfaces (72), and microparticles (66, 94, 95). **Figure 3*a*** illustrates DNA motors that traverse tracks consisting of a microparticle surface (66), a carbon nanotube (70), a DNA origami platform (71), and a gold-coated glass surface (72). In the case of DNA-based tracks, binding sites can be placed at regular intervals according to the helical pitch of dsDNA (10.5 bp or 3.5 nm) along a single-helix track, or at varied spacing along adjacent helices in DNA origami nanostructures. Recent advances in imaging of DNA walkers have led to improved quantification of motion and steps, including successful visualization of individual steps of walkers stepping on DNA origami tracks where binding sites are positioned ~6 nm apart (96, 97). Although the conceptual design of DNA walkers was inspired by natural biomolecular motors and the step sizes can be similar to, for example, kinesin, which takes 8-nm steps (98), their speeds are much slower. Typical speeds of nanoscale DNA motors range from ~1 to 10 nm/min (70, 92, 96, 99), whereas kinesin motors can move along microtubules at speeds of ~50 μm/min. Recently, DNA motors based on rolling of larger, micrometer-scale particles coated with DNA demonstrated speeds of up to ~1–5 μm/min (72). Significant research efforts are pursuing improvements in speed and control,

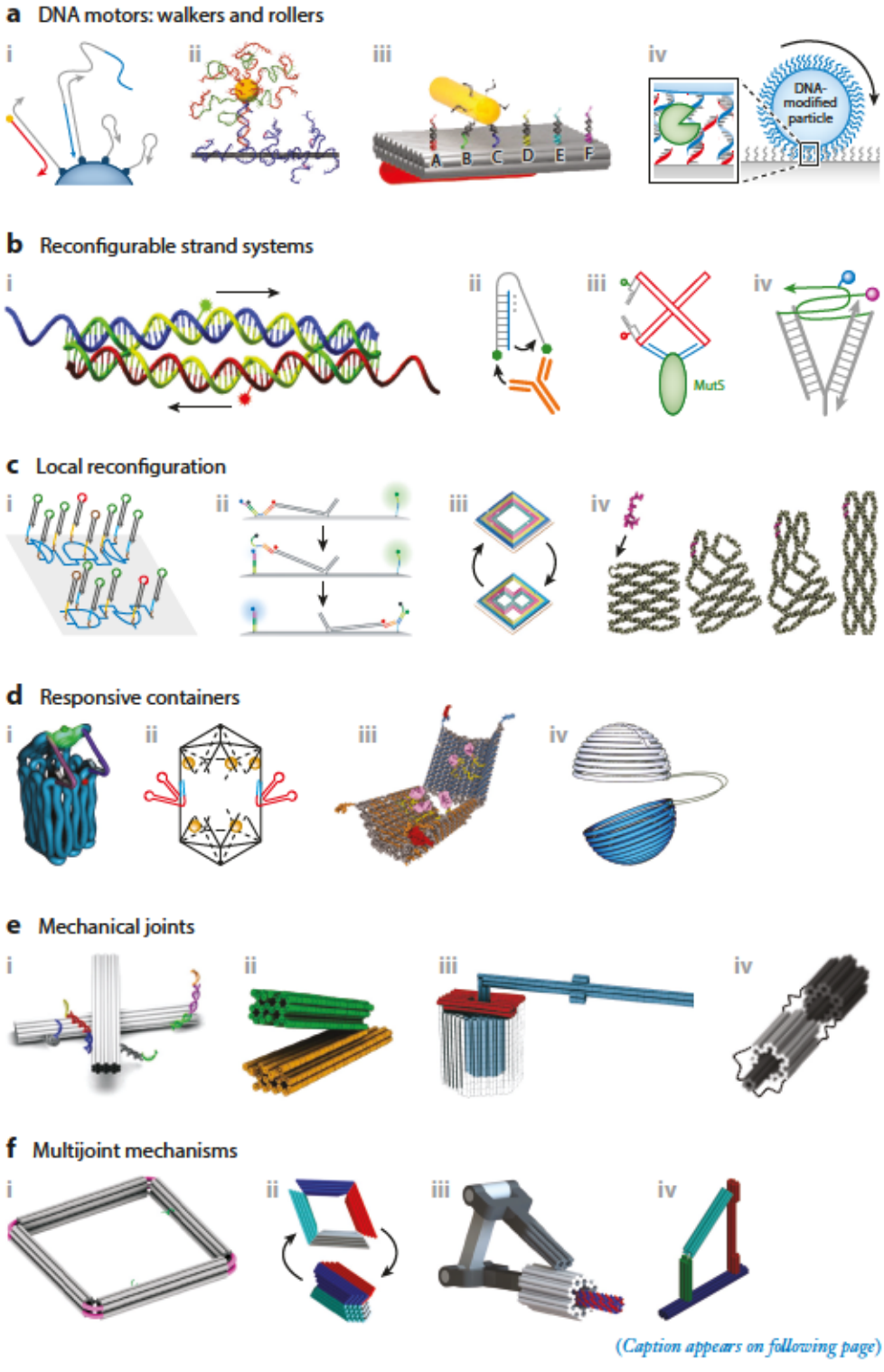

(Caption appears on following page)

Figure 3 *(Figure appears on preceding page)*

Classes of dynamic DNA nanodevices. (*a*) DNA motors proceed along tracks that can consist of (*i*) microparticles (66), (*ii*) carbon nanotubes (70), (*iii*) DNA origami platforms (71), or (*iv*) flat surfaces (72). Motors generally proceed along successive anchoring sites by stepping (walkers) or rolling (rollers), and in some cases motion may be achieved by some combination of the two. (*b*) Reconfigurable strand systems are similar in size to walkers, but generally change shape in response to specific cues such as (*i*) DNA strand displacement (73), (*ii*) binding of antibodies (74) or (*iii*) DNA-binding proteins (75), or (*iv*) changes in pH (76). These strand systems are often used as sensors such that shape changes lead to measurable readouts. (*c*) Strand-based devices can be mounted onto the structure or material platforms (*i*) to enhance strand interactions for molecular computation (77), (*ii*) to transport molecular cargo along a structure template (78), (*iii*) to reconfigure patterns in a template (79), or (*iv*) to communicate information by cascaded conformational changes (80). (*d*) Interest in exploiting dynamic DNA nanodevices for drug delivery has inspired nanoscale containers that can open in response to (*i*) DNA strand displacement (81), (*ii*) binding interactions between incorporated aptamers and target small molecules (82) or (*iii*) cell surface receptors (6), or (*iv*) externally applied light input (83). (*e*) More recently, a number of efforts have led to DNA nanodevices that resemble macroscopic mechanical joints, including (*i*) pin joints (84), (*ii*) hinge joints (85), (*iii*) rotor joints (86), and (*iv*) slider joints (87). (*f*) These joints can be integrated into mechanisms with more complex motions such as (*i*) two-dimensional (88) or (*ii*) three-dimensional (87) opening/closing of planar or spatial mechanisms, (*iii*) coupling between rotational and linear motion in a crank-slider mechanism (87), and (*iv*) bistable behavior of a mechanism that integrates a deformable, or compliant, component (89).

broad integration with other materials and structures, and enhancement and application of motor function.

Reconfigurable strand systems (**Figure 3*b***) are similar in size to typical DNA walkers, with dimensions on the ~1–10-nm scale, but are designed to undergo conformational changes in response to specific triggers such as DNA strand displacement (73), site-specific binding of biomolecules (74, 75), or changes in solution conditions such as pH (4, 76). This responsive function makes these strand-based devices powerful tools for sensing various biomolecules or environmental conditions. These devices have even been implemented in living cells to probe pH (4, 76) or detect ion concentrations (100), and they have been used in full organisms, such as *Caenorhabditis elegans*, to measure local pH (101). In addition, these devices can be functionalized with, for example, targeting moieties (76, 101, 102) or other aptamers that enable detection of specific molecular targets (103).

These reconfigurable strand elements can be mounted onto larger nanostructures or material templates (**Figure 3*c***) to provide local actuation, sensing, or communication elements or to enhance control or performance of the device function. For example, a recent study demonstrated a platform in which computations can be carried out via interactions between strands immobilized on a DNA origami nanostructure platform; localizing interacting strands on a static platform reduces the time for computation steps from hours to minutes compared with similar processes carried out in solution (**Figure 3*c*, *i***) (77). Simmel and colleagues (78) used reconfigurable strands to transport cargo on a DNA origami platform (**Figure 3*c*, *ii***). The ability to reconfigure strands in a larger template can also add functionality to the template, such as changing local structure patterns (**Figure 3*c*, *iii***) (79) or reconfiguring structures through the selective removal of entire layers (104). More recently, Song et al. (80) developed an approach to transmit information along DNA nanostructure via propagation of local conformational changes of structural units (**Figure 3*c*, *iv***). These controllable strand modules have recently been implemented within DNA crystals (105), suggesting that these devices can impart local function to macroscopic (~100-μm) material systems.

The ability to design complex geometry, in combination with reconfigurable and biochemically addressable components, offers the potential for drug delivery devices that can encapsulate

compounds and then release them by opening in response to environmental cues, for example, biomolecules that are indicative of disease states. With this goal in mind, investigators studying dynamic structural DNA nanotechnology have expended significant effort in developing responsive container-like structures, starting with an ~40-nm DNA origami box with a lid that can be opened via DNA strand displacement (106). **Figure 3*d*, *i*** depicts a smaller (~20-nm) box that can be repeatedly opened and closed through successive strand displacement steps (81). Other studies have exploited the biochemical specificity of DNA-based aptamers to create containers responsive to non-DNA triggers, such as small molecules involved in bacterial cell signaling (**Figure 3*d*, *ii***) (82) or cell surface receptors (**Figure 3*d*, *iii***) (6). In addition to responding to specific target molecules, a recent study demonstrated the ability to open a spherical DNA origami capsule by light actuation (**Figure 3*d*, *iv***) (83). Given recent advances in studies of the behavior of DNA nanostructures in vivo, including investigations showing effective stability and distribution (107, 108) as well as promising targeting (109) and tumor efficacy (110) in mice, this line of research is likely to be extended in the coming years with increasing emphasis on translational studies.

An emerging area of DNA nanotechnology involves the development of dynamic DNA origami nanodevices that exhibit well-defined mechanical motions, much like macroscopic machines and robots. These devices typically integrate multiple stiff bundle components whose relative motion is enabled by flexible ssDNA domains. These ssDNA connections can enable angular motion via pinlike connections between dsDNA bundle components (**Figure 3*e*, *i***) (84) or multiple short ssDNA connections arranged along a line to enable hinging motion around a defined axis of rotation (**Figure 3*e*, *ii***) (85, 111). As an alternative approach, relative motions of components can be achieved using close-fitting complementary geometries such as a rotor inside a stator (**Figure 3*e*, *iii***) (86). This approach of combining components with complementary geometries to constrain relative motion has also been used to enable piston-like linear motion via relative sliding of a tube along a track (**Figure 3*e*, *iv***) (87, 112).

These mechanical joints with specific types of motion can be integrated into multijoint mechanisms capable of more complex mechanical motion and function. For example, integration of four-bundle components with four hinge joints into a closed loop enables the construction of four-bar linkages that exhibit well-defined planar motions (**Figure 3*f*, *i***) (88). A recent study reported the construction of arrays of similar mechanisms to achieve shape-transforming 2D materials (113). More complex 3D transformations can be achieved by changing the orientations of angular degrees of freedom, as demonstrated by DNA origami Bennett linkage (**Figure 3*f*, *ii***) (87). Marras et al. (87) demonstrated the integration of angular and linear motion in a DNA origami crank-slider mechanism (**Figure 3*f*, *iii***) that couples translation of a slider component to hinge rotation, similar to crank-slider mechanisms that couple linear motion of a piston to rotation of a wheel in classic steam-locomotive trains.

Although the majority of machines utilize rigid components with highly flexible joints, the integration of deformable, or compliant, components (114) [i.e., compliant mechanism design (115)] has become a powerful approach in macroscopic mechanical design, offering advantages such as tunable mechanical properties, improved motion stability, and complex mechanical behavior such as bistability. Similarly, the integration of compliant components into DNA origami nanostructures has led to distributed deformation (116), tunable mechanical properties (114, 117), and programmable bistable behavior (**Figure 3*f*, *iv***) (89).

Exploiting these dynamic devices, in particular for nanorobotic systems, requires the ability to control their conformation. The mostly widely used approach to control dynamic nanodevices is via binding or displacement of DNA strand components, initially developed by Yurke et al. (118). The diversity and specificity of DNA sequences make this a highly versatile approach that can be used to achieve processive motion (**Figure 4*a*, *i***) (90) as discussed elsewhere for DNA

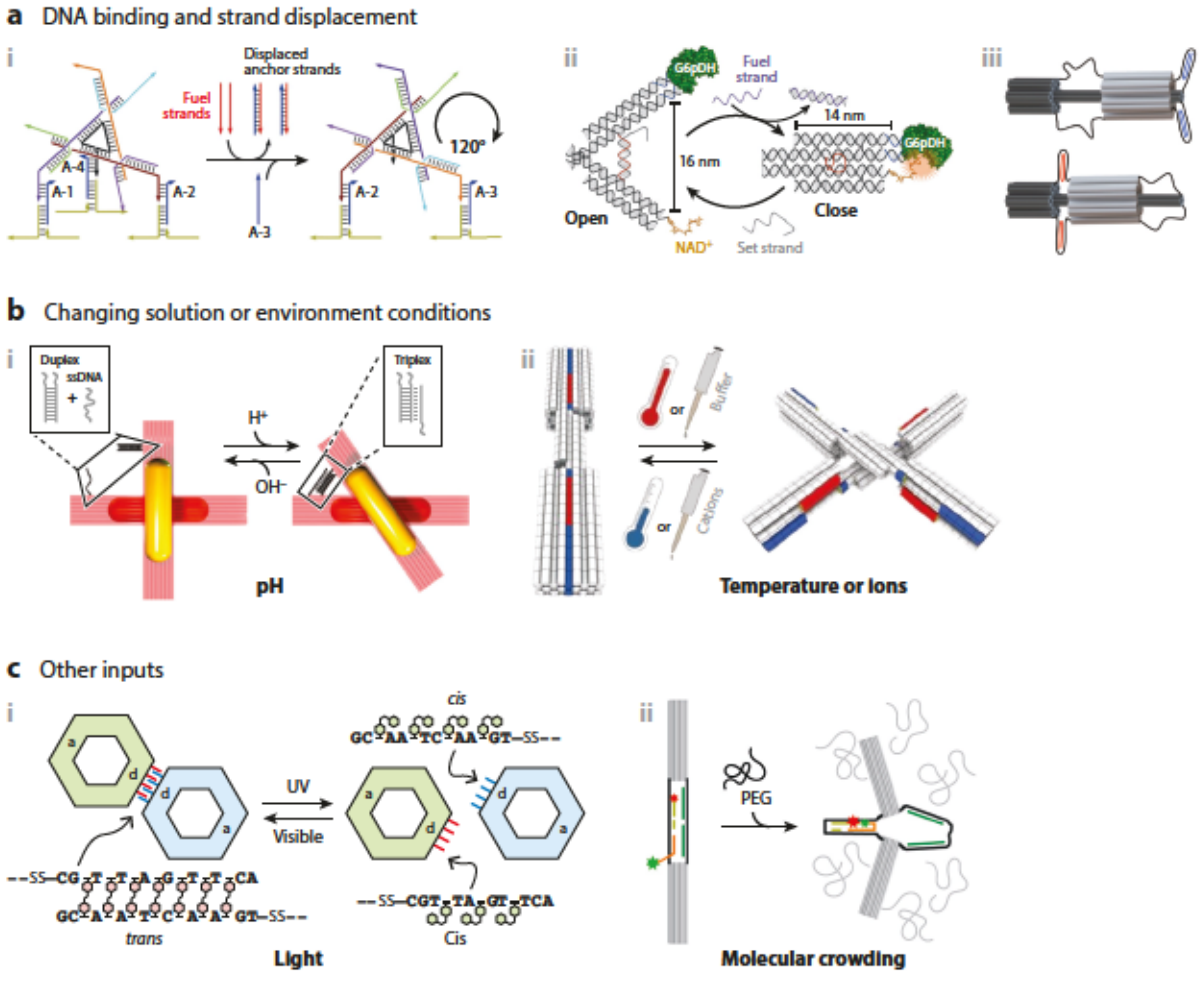

Figure 4

Actuation mechanisms for dynamic DNA nanodevices. (*a*) The most common approach to actuate DNA nanodevices is DNA binding or strand displacement to facilitate or release connections between components of the system, respectively. This approach enables (*i*) processive motion of DNA motors (A-1 through A-4 denote anchoring sites of the DNA motor) (90), (*ii*) opening and closing of hinge-like devices (119), or (*iii*) extension and retraction of a sliding joint (112). (*b*) To avoid the need to introduce DNA actuator strands, devices can be designed to be responsive to local solution conditions such as (*i*) pH to trigger formation of a triplex from a duplex and single-stranded DNA (ssDNA) (120) or (*ii*) temperature and ion concentrations to mediate local interactions that stabilize a closed state (113). These approaches generally enable faster, repeatable, and potentially less invasive control mechanisms. (*c*) Other mechanisms for controlling DNA nanodevices include (*i*) photoactivation, for example, to reversibly control assembly of multiple structures (SS indicates a disulfide bond that connects the photoswitchable overhang strand to the structure) (121), and (*ii*) molecular crowding, which can bias a dynamic device into a compacted state (122). Abbreviations: G6pDH, glucose-6-phosphate dehydrogenase; PEG, poly(ethylene glycol); NAD^+, nicotinamide adenine dinucleotide; ssDNA, single-stranded DNA.

motors, strand reconfiguration (73, 118), angular motion (**Figure 4*a*, *ii***) (119), linear motion (**Figure 4*a*, *iii***) (112), and container opening and closing (81, 106). Because it is easy to incorporate ssDNA strands at specific locations on DNA nanostructures, nearly any dynamic DNA device can be actuated via DNA strand binding and/or displacement (123). However, limitations, especially the relatively slow response times (minutes or greater) (124) and the need to introduce new

strands into solution for every actuation step, have led to the development of other control methods, such as pH-controlled reversible latching of components (**Figure 4*b*, *i***) (120) or regulation of weak base-stacking interactions of shape-complementary components via changes in temperature or ion conditions (**Figure 4*b*, *ii***) (113), both of which offer response times on the ~10-s scale. Temperature has the advantage of being easily adjusted without the need to change the solution environment, which means that it is straightforward to reverse and repeat the actuation via cyclic temperature changes. Gerling et al. (113) illustrated actuation via temperature changes over ~1,000 cycles. Similarly, light-mediated actuation can be used as an external input to reconfigure devices (125), control the position of a rotor (126), actuate DNA walkers (97), or control assembly and disassembly (**Figure 4*c*, *i***) (121). Most of these photoactuated devices incorporated azobenzene units along latching strands, where UV-driven *trans*-to-*cis* conformation change destabilizes hybridized strands (127), although some studies have incorporated photocleavable molecules (83). Another recent study demonstrated that dynamic closing of a device can be driven by molecular crowding (**Figure 4*c*, *ii***) (122). Although this approach requires changing the solution conditions, it may give rise to devices that can respond to changing environments in biological systems, such as inside cells. Additionally, recent research has demonstrated a nanodevice that can reconfigure upon interaction with a lipid bilayer (128), which may enable the construction of DNA devices that interact with biological membranes.

Various stimulus response mechanisms have been developed, but major challenges in controlling dynamic nanodevices remain. Although methods including temperature- and pH-mediated actuation have led to faster response times, down to ~10 s, these response times are still much slower than inherent fluctuation times, suggesting that DNA devices could be reconfigured with significantly faster methods. In addition, existing control methods simply trigger the structure between a freely fluctuating state and a single, preprogrammed, closed or latched state. The ability to achieve continuous control over a wide range of conformations remains a challenge. Lastly, the effects of force on actuation have not been studied; such investigations are necessary in order to consider the possibility of force-generating DNA actuators and motors. Because many processes rely on random thermal fluctuations, more advanced methods may be required to overcome or generate any significant forces.

The use of biological molecular motors may present solutions to some of these challenges or enable new applications for DNA devices. Although at present it is difficult to achieve function similar to that of natural motors, particularly in terms of kinetic rates and chemical fuel sources, one can draw interesting and useful analogies by comparison. In some cases, such as in DNA walkers, designs are directly inspired by molecular motors such as myosin (**Figure 5**) (63, 129). Some functional features, such as coordination between track-binding domains, have already been explored (64, 65), and other features, such as mechanical communication between motorheads (130) or long linkers between motor body and the motorheads (i.e., binding domain), could provide useful design inspiration. Freely rotating DNA devices (86) undergo similar motions to biological rotary motors such as F1-ATPase (**Figure 5*b***) (131), but they are limited in terms of directional rotation and rotation speeds; similarly, sliders that can travel relatively long distances along DNA origami tracks (132) are similar in geometric and motion design to DNA translocating motors such the bacteriophage T4 portal protein (**Figure 5*b***) (133). Lastly, DNA origami hinges can be similar in size and shape to proteins like condensins or cohesins (134), which regulate chromatin structure, or the monopolin complex (**Figure 5*b***) (135), which regulates attachments between kinetochores and microtubules in fungi. Given recent uses of DNA origami nanodevices to engage and study nucleosomes (136, 137), dynamic nanodevices could find application in regulating the structure of chromatin or other large biomolecular complexes and materials.

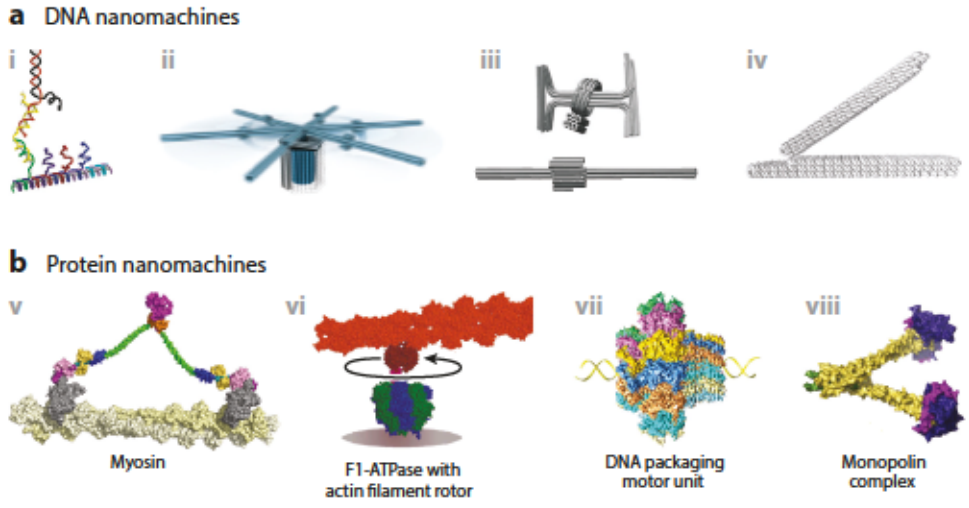

Figure 5

(*a*) DNA nanodevices and (*b*) biomolecular design analogs. (*i*) DNA walkers (63) are directly inspired by biomolecular motors such as myosin (*v*) (129). These biological motors provide functional guidance that could enhance DNA motor function, or continue inspiration for new applications. DNA assemblies that incorporate components that fit together for (*ii*) rotary (86) or (*iii*) linear (132) motion are similar in geometric design to (*vi*) F1-ATPase (131) or (*vii*) DNA translocating motors (133), which could serve as inspiration for new mechanisms to achieve relative motion of tight-fitting components. (*iv*) DNA origami hinges (87) are similar in size scale and motion characteristics to proteins such as (*viii*) the monopolin complex (135) that regulate chromatin interactions or structure. These protein complexes may provide useful concepts with which to develop DNA nanodevices that control the structure of chromatin or other large macromolecular complexes.

3. BIOMEDICAL APPLICATIONS OF DNA NANOSTRUCTURES

As discussed above, complex static and dynamic nanostructures of arbitrary geometries may be constructed via DNA self-assembly. These DNA nanostructures have been explored for diverse biological and biomedical applications for several reasons. First, because the nanostructures are made from DNA, they are intrinsically biocompatible. Second, DNA structures, especially origami, can be utilized as nanoscale breadboards because they exhibit extremely high addressability. Roughly 200 staple oligonucleotides work cooperatively with a long-chain scaffold strand, forming an origami structure. The staple strands may be used for grafting and organizing biomolecules including nucleic acids, proteins, and nanoparticles. Third, individual DNA strands within DNA nanostructures may be further modified chemically if necessary. For example, there is a plethora of organic fluorophores and photoresponsive moieties (such as azobenzene) that may be functionalized in DNA strands. Such functionality and chemical versatility make DNA ideal for use in diverse applications.

Given these unique advantages, DNA nanostructures have been explored for (*a*) biomolecular sensing, (*b*) both in vitro and in vivo imaging, and (*c*) drug delivery applications. In this section, we discuss how DNA nanostructures can be used in such applications. As several in-depth reviews on each of these applications are available elsewhere (e.g., 138), this overview highlights how static and dynamic DNA nanostructures are exploited distinctly. We focus on the unique aspects of self-assembly and programmability that enable static and dynamic structures for the applications. We do not discuss studies of DNA computations inside cells (139) or biomolecular sensors based on simple DNA-based molecular beacons (140, 141) and origami-based nanopores (142).

3.1. Biomolecular Sensing: Optical Detection and Atomic Force Microscopy Measurements

Biomolecular sensors are composed of target recognition elements and signal transducers integrated into DNA nanostructures. Dynamic DNA structures reconfigure their conformations in response to analyte recognition, where shape-changing events are used as signal readouts, often with atomic force microscopy (AFM). In contrast, static structures are used as platforms where target binding events are recorded via direct AFM measurements of target molecules or indirect remote measurements using, for instance, fluorescence resonance energy transfer (FRET)-based optical detection. The recognition elements typically rely on target–ligand binding interactions. The ligands are often nucleic acids, aptamers, and antibody proteins.

Figure 6 shows examples of biomolecular sensing using static DNA nanostructures. Endo & Sugiyama (143) constructed origami rectangles with square holes at the center and two DNA cantilevers bridged across the holes (**Figure 6*a***). They used this platform in a series of studies to investigate the dynamic motions and kinetics of biomolecular analytes at the single-molecule level with high-speed AFM. For example, DNA binding events such as DNA base pairing, guanine quadruplex formation, and DNA–enzyme binding resulted in association or dissociation of the cantilever bridges (e.g., Holliday junctions) that was detected by AFM. Similar schemes were used to detect B–Z transitions of DNA strands as a function of Mg^{2+} concentration and to demonstrate photoregulated DNA base pairing using photoisomerizable azobenzene moieties.

The programmability and addressability of DNA origami structures have been demonstrated for a label-free hybridization assay (**Figure 6*b***). Yan and colleagues (144) constructed an origami rectangle containing three different probes arranged in a spatially resolved fashion. The capture of target RNA strands by the probes stiffened the probes, which could then be detected by AFM. This study exemplifies the simple yet powerful approach of DNA nanostructures, leading to the development of other DNA assembly–based biosensors.

In dynamic biosensor schemes, structural reconfigurations are associated with analyte binding events (**Figure 7**). A popular sensor design is a scissor/plier-type structure, which was demonstrated independently by multiple groups. Kuzuya et al. (145) first created single-molecule beacons from DNA origami that pinch closed upon binding to a target molecule (**Figure 7*a***). They also demonstrated unzipping by target binding. This design enabled examination of various analytes, including streptavidin, immunoglobulin G, telomere strands, microRNA (miRNA), and ATP. The structural changes were detected by AFM and fluorescence measurements. A similar structural design was adopted by Niemeyer and colleagues (146), who investigated analyte binding kinetics (**Figure 7*b***).

The Yan group (147) expanded this concept to construct a DNA tweezer that pinches near a fuel strand, initiating a NAD^+/NADH reaction by glucose-6-phosphate dehydrogenase (**Figure 7*c***). The reconfiguration dynamics were characterized by recording fluorescence signals from a by-product molecule and a FRET pair. **Figure 7*d*** shows a nanomechanical origami device capable of long-range allosteric activation, proposed by Ke et al. (88). Four rigid rods are connected by flexible single-stranded hinges, allowing reconfiguration of the entire structure via allosteric changes upon recognition of analyte molecules. Such dynamic nanodevices should become useful in biosensing and single-molecule biophysics studies.

3.2. Cellular Imaging

Cellular imaging with DNA probes and DNA imaging inside cells are routinely performed in biological and biomedical research. DNA strands are typically tagged or modified with radioactive

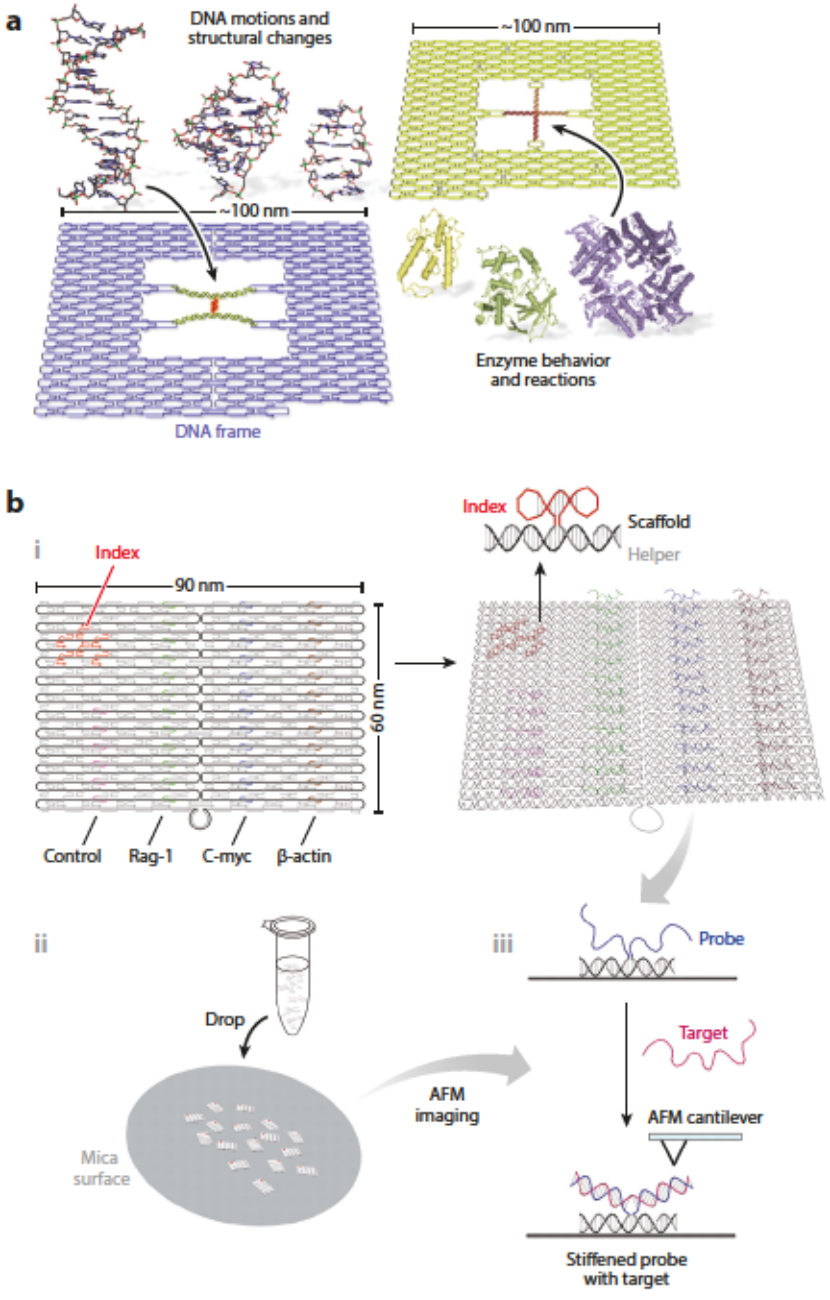

Figure 6

Static DNA nanostructures for biomolecular sensing. (*a*) Single-molecule biosensing and biophysics platform (143). (*b*) DNA origami–based label-free RNA hybridization assay (144). Abbreviation: AFM, atomic force microscopy.

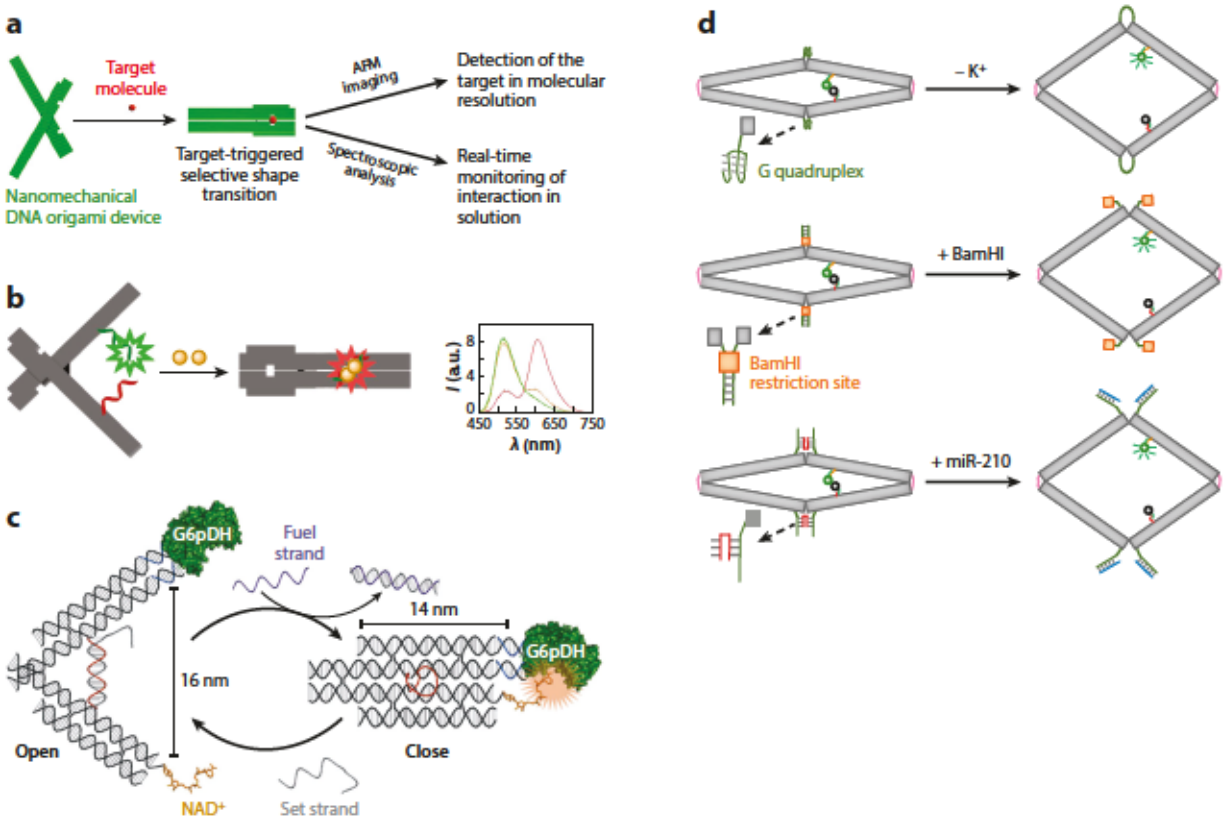

Figure 7

Examples of dynamic DNA nanostructures that reconfigure their conformations in response to analyte recognition. (*a*,*b*) Nanopliers as a single-molecule sensing platform (145, 146). The DNA plier pinches closed or open upon target binding. (*c*) Enzymatic nanoreactor enabled by reconfigurable DNA assemblies (147). (*d*) Biosensing via allosteric activation (88). Abbreviations: AFM, atomic force microscopy; BamHI, a type II restriction endonuclease from *Bacillus amyloliquefaciens*; G6pDH, glucose-6-phosphate dehydrogenase; miR-210, a short microRNA; NAD^+, an oxidized form of nicotinamide adenine dinucleotide (NAD).

or fluorescent moieties for imaging. In particular, optical imaging with fluorophore-tagged DNA strands is one of the most common methods for cellular imaging, and it is possible to achieve spatial resolution far below the fundamental diffraction limit (~λ/2)—so-called superresolution microscopy. Notably, DNA nanotechnology offers unique advantages with unprecedented predictability and programmability that allow us to move beyond current microscopy techniques. For example, one of the most critical limitations in stochastic subdiffraction imaging is the availability of photoswitchable fluorophores with desirable spectroscopic characteristics.

To address this issue, Jungmann et al. (148, 149) employed a simple yet powerful technique involving a new type of superresolution fluorescence microscopy that uses transient binding of regular fluorophore-tagged oligonucleotides onto DNA origami structures for localization. Diffusing imager strands bind transiently and repetitively to the complementary docking strands on the origami, thus switching continuously between on and off states (**Figure 8*a***). In this DNA-based point accumulation for imaging in nanoscale topography (DNA-PAINT) scheme, photobleaching can be overcome. The authors extended this approach by integrating antibodies to the docking strands so that different parts of cells could be imaged with a single type of

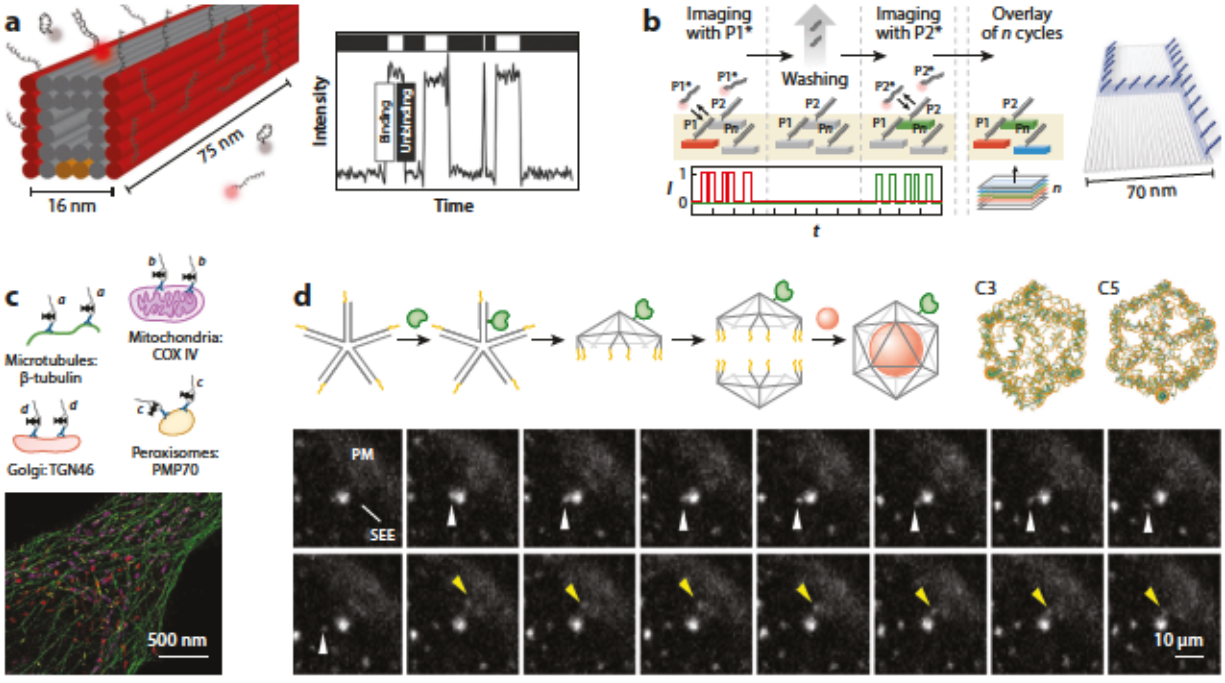

Figure 8

DNA nanostructures as optical probes for cellular imaging. Principles of (*a*) DNA-based point accumulation for imaging in nanoscale topography (DNA-PAINT) and (*b*) Exchange-PAINT (148, 149). (*c*) Multiplexed imaging of a fixed HeLa cell using Exchange-PAINT. (*d*) Single-particle tracking inside cells with DNA nanocages that contain nanoparticles (150). Rendering of an icosahedron showing the C3 and C5 axes of symmetry. Each white arrowhead points to a fission event that results in a small dynamic endosome. Each yellow arrowhead denotes a vesicle fusion event of the plasma membrane with a static early endosome. Abbreviations: COX IV, cytochrome *c* oxidase subunit 4, isoform 1; *I*, normalized intensity; PMP70, adenosine triphosphate–binding cassette subfamily D, member 3; P*n*, *n*th docking strand; P1/P1*, first docking strand/imager strand; P2/P2*, second docking strand/imager strand; *t*, time; TGN46, *trans*–Golgi network integral membrane protein.

fluorophore. Here, one set of imager strands was first imaged and washed, then exchanged with another set for another run of imaging that could be repeated for different cellular components (a technique known as Exchange-PAINT) to achieve multiplexed imaging (**Figure 8*b***). The authors successfully demonstrated this concept in fixed cells (**Figure 8*c***) and reported sub-10-nm spatial resolution. The Krishnan group (150) proposed another novel technique for cellular imaging by integrating the programmability of DNA nanostructures and the photostability of nanocrystal quantum dots (QDs) that have superior photoproperties compared with those of conventional fluorescent proteins and organic dyes. These authors encapsulated a QD inside DNA icosahedra for single-particle tracking (SPT) to investigate endocytosis (**Figure 8*d***). Endocytic ligands were attached to the DNA icosahedra, and the individual particles were imaged during the cellular uptake process used to study endocytic pathways.

In addition to performing SPT studies with DNA nanocages, the Krishnan group (4, 150) has proposed the use of dynamic, reconfigurable DNA structures for cellular imaging (**Figure 9**). These DNA nanostructures are responsive to the change of pH in the local environment, reconfiguring their conformations to open at high pH and close at low pH. This pH-responsive behavior can be exploited in conjunction with FRET for spatiotemporal mapping of cellular components in

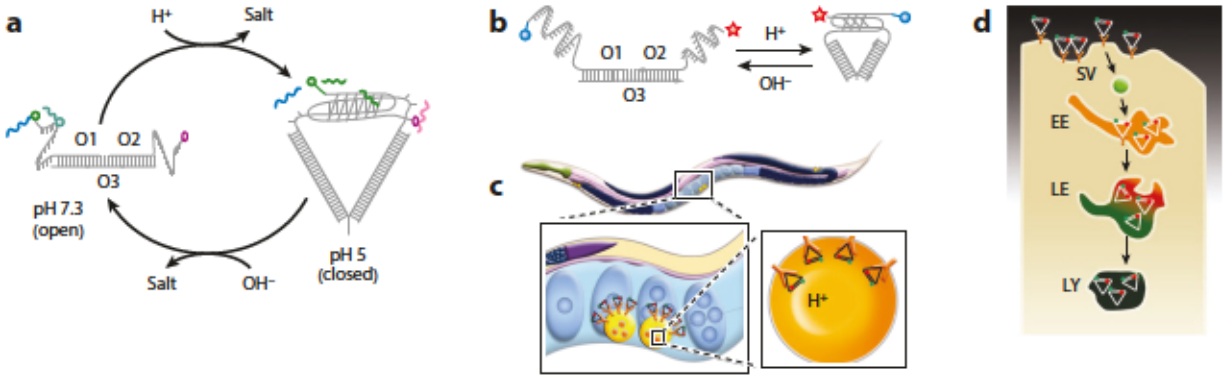

Figure 9

Dynamic DNA nanostructures for cellular imaging proposed by the Krishnan group (4, 150). (*a*,*b*) The structures reconfigure their conformations in response to a change of pH in the local environment, which is used to image (*c*) cell components and (*d*) endocytic processes in living organisms. Three oligonucleotides are labeled O1, O2, and O3, where O1 and O2 are hybridized to flanking sequences on O3. Abbreviations: EE, early endosome; LE, late endosome; LY, lysosome; SV, spherical vesicle.

organisms (*Drosophila* and *C. elegans*). The authors further developed this concept by integrating two pH-responsive DNA nanomachines to visualize and study distinct endocytic pathways (101).

3.3. Drug Delivery and Therapeutics

Drug delivery and therapeutics represent one of the most promising applications of structural DNA nanotechnology. Several studies have proposed various structures and strategies to load, deliver, and release molecular drugs for cancer treatment, gene silencing, immunostimulation, and photodynamic therapy. The general schemes proposed in these studies involve the use of DNA nanostructures loaded with disease/function-specific agents and ligands to locate the target location, followed by the release of the agents from the structures to complete the intended tasks. As described above, the proposed DNA assemblies may be classified into static and dynamic structures.

The most common use of static DNA structures in therapeutics is anticancer drug delivery. In 2012, the Ding group (151) and the Högberg group (152) independently constructed DNA origami structures incorporating the anticancer drug doxorubicin (DOX) via intercalation (**Figure 10*a***). The drug-loaded DNA structures were incubated with and internalized by human breast cancer cells, which clearly demonstrated apoptotic behavior. Both groups demonstrated efficient drug delivery and the efficacy of the anticancer treatment as a function of dosage. In a later study, Ding and collaborators (153) examined origami-based anticancer drug carriers in small animals (**Figure 10*b***). The origami structures were decorated with QDs whose fluorescence properties were used to investigate biodistribution and pharmacokinetics. The DOX was demonstrated to be effective in vivo and had no measurable cytotoxic effects.

DNA structures have been explored for biomedical applications in addition to cancer therapy. The Liedl group (154) examined the feasibility of DNA structures for immunostimulant delivery to immune cells (**Figure 10*c***). They prepared DNA nanotubes containing CpG sequences and examined their effects in spleen cells. Their findings show that the carriers have no significant toxicity and that their immunological behavior functioned as designed (154). In another study, Langer and colleagues (109) used tetrahedral DNA oligonucleotide nanoparticles (ONPs) as vehicles for small-interfering RNA delivery (**Figure 10*d***). They successfully demonstrated silencing of target genes in small animal models.

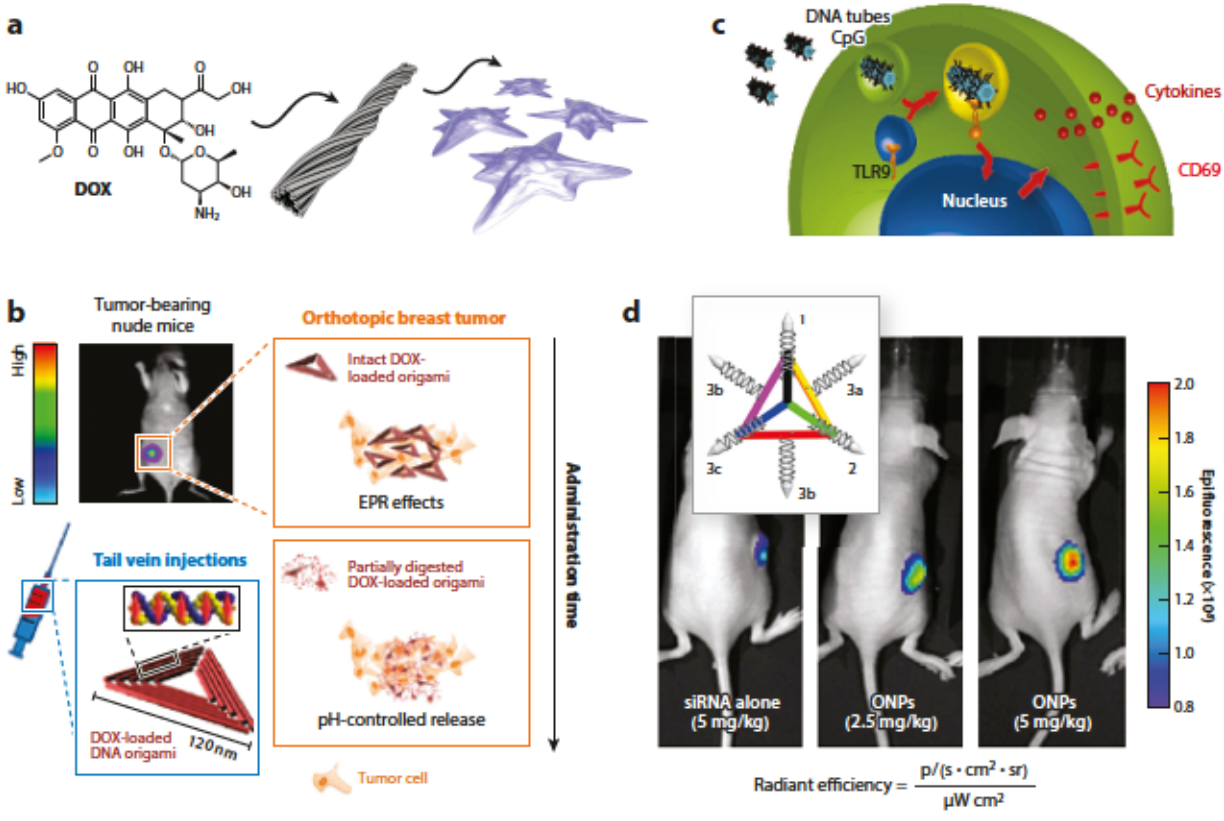

Figure 10

Static DNA nanostructures for drug delivery and therapeutics. (*a*) Anticancer drug DOX-loaded DNA origami for human cancer treatment (152). (*b*) Self-assembled DNA triangles for in vivo cancer therapy (151). (*c*) Delivery of immunostimulants (154). (*d*) DNA tetrapod for small interfering RNA (siRNA) delivery in vivo (109). Abbreviations: CD69, cluster of differentiation 69; CpG, cytosine–phosphate–guanine; DOX, doxorubicin; EPR effect, enhanced permeability and retention effect; ONP, oligonucleotide nanoparticle; TLR9, Toll-like receptor 9.

Compared with static delivery vehicles, dynamic DNA nanostructures offer another critical advantage: programming the availability of drugs. Gothelf and colleagues (36) designed a DNA origami box that opens or closes its lid only when specific external cues are recognized. With the lid open, the payload inside the box becomes available (**Figure 11*a***). Such dynamic structures present significant advantages over static structures, which cannot control the availability of drug molecules.

This concept was implemented by Douglas et al. (6), who designed an origami barrel capable of opening and closing in response to recognition of specific cues (**Figure 11*b***). When a box loaded with a cocktail of molecular agents is presented to cells, aptamer-encoded logic gate units on the barrel interact with receptors on the cells' surface, opening the lid and making the molecular payloads available for release. The authors confirmed the robustness of this approach with various cell lines, including Jurkat cells and human T lymphocyte cells. The reconfigurable DNA nanostructures may be further developed as delivery vehicles if novel release mechanisms such as external light irradiation are programmed. For example, two research groups led by Han (155) and Choi (156) separately demonstrated photoactivated mechanisms that release molecules

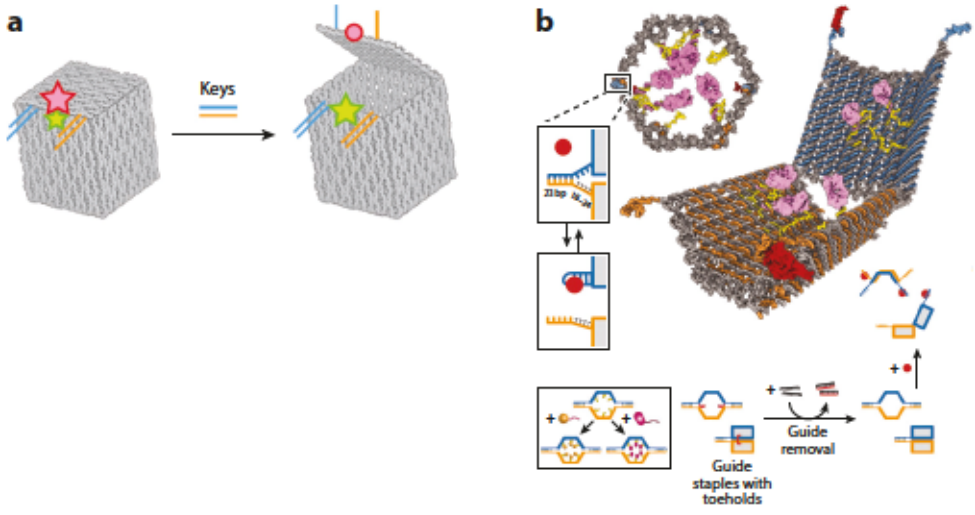

Figure 11

Dynamic DNA nanostructures for drug delivery. DNA origami containers open their lid upon cues and release the loaded drug molecules. (*a*) Schematic of a DNA origami box that opens and closes its lid in response to binding to a molecular target, demonstrated by Gothelf and colleagues (36). (*b*) Schematics of an origami based delivery system loaded with drug payloads by Douglas et al. (6). Recognition of a target analyte by DNA aptamers releases the lock, making the payloads available.

from DNA origami. Thus, it will become possible to design DNA nanorobots that can sense the environment, locate the target area, open up the structure, and release payloads.

4. CONCLUSIONS

Both static and dynamic DNA nanostructures have presented tremendous opportunities in biomedical research. These structures offer a set of properties that set them apart from conventional materials used in biomedical applications, including (*a*) precise controllability over nanostructures' physicochemical properties (e.g., size, shape, surface functionality); (*b*) programmability of sensing, computing, and responding to external stimuli (e.g., light, pH, biomarkers); (*c*) biological functionality (e.g., interaction with cellular proteins and genetic nucleic acids); and (*d*) biocompatibility and biodegradability. Although recent advances in DNA nanotechnology have demonstrated many exciting biomedical applications, the field is still in its infancy and is facing many challenges that hinder its translation to biomedical research. These challenges include but are not limited to the following:

1. Immunogenicity. Like many foreign materials, DNA nanostructures may trigger an unwanted immune response. Chemical modification of the bases and backbone could mitigate this issue.
2. Off-target gene regulation. DNA strands may contain certain sequences that nonspecifically regulate gene expressions by interacting with messenger RNAs, miRNAs, or genes. Rationally optimizing the sequence and chemically modifying the DNA may lower the risk of nonspecific gene regulations.
3. Pharmacokinetics and pharmacodynamics. The pharmacokinetic and pharmacodynamic profiles of DNA nanostructures are unclear. Both will be essential for in vivo applications of DNA nanostructures and require further investigation.

4. Expense. DNA is more expensive than alternative materials, such as polymers. More economical production of DNA is under active study.

DISCLOSURE STATEMENT

The authors are not aware of any affiliations, memberships, funding, or financial holdings that might be perceived as affecting the objectivity of this review.

LITERATURE CITED

1. Watson JD, Crick FH. 1953. Molecular structure of nucleic acids: a structure for deoxyribose nucleic acid. *Nature* 171:737–38
2. Shipman SL, Nivala J, Macklis JD, Church GM. 2017. CRISPR-Cas encoding of a digital movie into the genomes of a population of living bacteria. *Nature* 547:345–49
3. Seeman NC. 1982. Nucleic acid junctions and lattices. *J. Theor. Biol.* 99:237–47
4. Modi S, Swetha MG, Goswami D, Gupta GD, Mayor S, Krishnan Y. 2009. A DNA nanomachine that maps spatial and temporal pH changes inside living cells. *Nat. Nanotechnol.* 4:325–30
5. Jungmann R, Avendano MS, Woehrstein JB, Dai MJ, Shih WM, Yin P. 2014. Multiplexed 3D cellular super-resolution imaging with DNA-PAINT and Exchange-PAINT. *Nat. Methods* 11:313–18
6. Douglas SM, Bachelet I, Church GM. 2012. A logic-gated nanorobot for targeted transport of molecular payloads. *Science* 335:831
7. Kallenbach NR, Ma RI, Seeman NC. 1983. An immobile nucleic-acid junction constructed from oligonucleotides. *Nature* 305:829–31
8. Ma RI, Kallenbach NR, Sheardy RD, Petrillo ML, Seeman NC. 1986. Three-arm nucleic acid junctions are flexible. *Nucleic Acids Res.* 14:9745–53
9. Wang YL, Mueller JE, Kemper B, Seeman NC. 1991. Assembly and characterization of five-arm and six-arm DNA branched junctions. *Biochemistry* 30:5667–74
10. Wang X, Seeman NC. 2007. Assembly and characterization of 8-arm and 12-arm DNA branched junctions. *J. Am. Chem. Soc.* 129:8169–76
11. Fu TJ, Seeman NC. 1993. DNA double-crossover molecules. *Biochemistry* 32:3211–20
12. Winfree E, Liu F, Wenzler LA, Seeman NC. 1998. Design and self-assembly of two-dimensional DNA crystals. *Nature* 394:539–44
13. Yan H, Park SH, Finkelstein G, Reif JH, LaBean TH. 2003. DNA-templated self-assembly of protein arrays and highly conductive nanowires. *Science* 301:1882–84
14. He Y, Chen Y, Liu H, Ribbe AE, Mao C. 2005. Self-assembly of hexagonal DNA two-dimensional (2D) arrays. *J. Am. Chem. Soc.* 127:12202–3
15. He Y, Tian Y, Ribbe AE, Mao C. 2006. Highly connected two-dimensional crystals of DNA six-point-stars. *J. Am. Chem. Soc.* 128:15978–79
16. He Y, Ye T, Su M, Zhang C, Ribbe AE, et al. 2008. Hierarchical self-assembly of DNA into symmetric supramolecular polyhedra. *Nature* 452:198–201
17. Zhang C, Su M, He Y, Zhao X, Fang PA, et al. 2008. Conformational flexibility facilitates self-assembly of complex DNA nanostructures. *PNAS* 105:10665–69
18. Zheng J, Birktoft JJ, Chen Y, Wang T, Sha R, et al. 2009. From molecular to macroscopic via the rational design of a self-assembled 3D DNA crystal. *Nature* 461:74–77
19. Ke YG, Ong LL, Shih WM, Yin P. 2012. Three-dimensional structures self-assembled from DNA bricks. *Science* 338:1177–83
20. Wei B, Dai MJ, Yin P. 2012. Complex shapes self-assembled from single-stranded DNA tiles. *Nature* 485:623–26
21. Zhang C, Wu W, Li X, Tian C, Qian H, et al. 2012. Controlling the chirality of DNA nanocages. *Angew. Chem. Int. Ed. Engl.* 51:7999–8002
22. Ke Y, Ong LL, Sun W, Song J, Dong M, et al. 2014. DNA brick crystals with prescribed depths. *Nat. Chem.* 6:994–1002

23. Tian C, Li X, Liu Z, Jiang W, Wang G, Mao C. 2014. Directed self-assembly of DNA tiles into complex nanocages. *Angew. Chem. Int. Ed. Engl.* 53:8041–44
24. Wang P, Wu S, Tian C, Yu G, Jiang W, et al. 2016. Retrosynthetic analysis–guided breaking tile symmetry for the assembly of complex DNA nanostructures. *J. Am. Chem. Soc.* 138:13579–85
25. Zhang C, Ko SH, Su M, Leng Y, Ribbe AE, et al. 2009. Symmetry controls the face geometry of DNA polyhedra. *J. Am. Chem. Soc.* 131:1413–15
26. He Y, Su M, Fang PA, Zhang C, Ribbe AE, et al. 2010. On the chirality of self-assembled DNA octahedra. *Angew. Chem. Int. Ed. Engl.* 49:748–51
27. He Y, Tian Y, Chen Y, Deng Z, Ribbe AE, Mao C. 2005. Sequence symmetry as a tool for designing DNA nanostructures. *Angew. Chem. Int. Ed. Engl.* 44:6694–96
28. Zhang F, Liu Y, Yan H. 2013. Complex Archimedean tiling self-assembled from DNA nanostructures. *J. Am. Chem. Soc.* 135:7458–61
29. Zhang F, Jiang S, Li W, Hunt A, Liu Y, Yan H. 2016. Self-assembly of complex DNA tessellations by using low-symmetry multi-arm DNA tiles. *Angew. Chem. Int. Ed. Engl.* 55:8860–63
30. Rothemund PWK. 2006. Folding DNA to create nanoscale shapes and patterns. *Nature* 440:297–302
31. Yan H, LaBean TH, Feng L, Reif JH. 2003. Directed nucleation assembly of DNA tile complexes for barcode-patterned lattices. *PNAS* 100:8103–8
32. Shih WM, Quispe J, Joyce G. 2004. A 1.7-kilobase single-stranded DNA that folds into a nanoscale octahedron. *Nature* 427:618–21
33. Ke YG, Douglas SM, Liu MH, Sharma J, Cheng AC, et al. 2009. Multilayer DNA origami packed on a square lattice. *J. Am. Chem. Soc.* 131:15903–8
34. Douglas SM, Dietz H, Liedl T, Högberg B, Graf F, Shih WM. 2009. Self-assembly of DNA into nanoscale three-dimensional shapes. *Nature* 459:414–18
35. Ke YG, Voigt NV, Gothelf KV, Shih WM. 2012. Multilayer DNA origami packed on hexagonal and hybrid lattices. *J. Am. Chem. Soc.* 134:1770–74
36. Andersen ES, Dong M, Nielsen MM, Jahn K, Subramani R, et al. 2009. Self-assembly of a nanoscale DNA box with a controllable lid. *Nature* 459:73–76
37. Ke Y, Sharma J, Liu M, Jahn K, Liu Y, Yan H. 2009. Scaffolded DNA origami of a DNA tetrahedron molecular container. *Nano Lett.* 9:2445–47
38. Han D, Pal S, Nangreave J, Deng Z, Liu Y, Yan H. 2011. DNA origami with complex curvatures in three-dimensional space. *Science* 332:342–46
39. Dietz H, Douglas SM, Shih WM. 2009. Folding DNA into twisted and curved nanoscale shapes. *Science* 325:725–30
40. Han D, Pal S, Yang Y, Jiang S, Nangreave J, et al. 2013. DNA gridiron nanostructures based on four-arm junctions. *Science* 339:1412–15
41. Zhao Z, Yan H, Liu Y. 2010. A route to scale up DNA origami using DNA tiles as folding staples. *Angew. Chem. Int. Ed. Engl.* 49:1414–17
42. Liu W, Zhong H, Wang R, Seeman NC. 2011. Crystalline two-dimensional DNA-origami arrays. *Angew. Chem. Int. Ed. Engl.* 50:264–67
43. Zhao Z, Liu Y, Yan H. 2011. Organizing DNA origami tiles into larger structures using preformed scaffold frames. *Nano Lett.* 11:2997–3002
44. Zhang HL, Chao J, Pan D, Liu HJ, Huang Q, Fan CH. 2012. Folding super-sized DNA origami with scaffold strands from long-range PCR. *Chem. Commun.* 48:6405–7
45. Iinuma R, Ke Y, Jungmann R, Schlichthaerle T, Woehrstein JB, Yin P. 2014. Polyhedra self-assembled from DNA tripods and characterized with 3D DNA-PAINT. *Science* 344:65–69
46. Marchi AN, Saaem I, Vogen BN, Brown S, LaBean TH. 2014. Toward larger DNA origami. *Nano Lett.* 14:5740–47
47. Benson E, Mohammed A, Gardell J, Masich S, Czeizler E, et al. 2015. DNA rendering of polyhedral meshes at the nanoscale. *Nature* 523:441–44
48. Gerling T, Wagenbauer KF, Neuner AM, Dietz H. 2015. Dynamic DNA devices and assemblies formed by shape-complementary, non–base pairing 3D components. *Science* 347:1446–52
49. Zhang F, Jiang S, Wu S, Li Y, Liu Y, Mao C. 2015. Complex wireframe DNA origami nanostructures with multi-arm junction vertices. *Nat. Nanotechnol.* 10:779–84

50. Liu W, Halverson J, Tian Y, Tkachenko AV, Gang O. 2016. Self-organized architectures from assorted DNA-framed nanoparticles. *Nat. Chem.* 8:867–73
51. Veneziano R, Ratanalert S, Zhang K, Zhang F, Yan H, et al. 2016. Designer nanoscale DNA assemblies programmed from the top down. *Science* 352:1534–48
52. Wang P, Gaitanaros S, Lee S, Bathe M, Shih WM, Ke Y. 2016. Programming self-assembly of DNA origami honeycomb two-dimensional lattices and plasmonic metamaterials. *J. Am. Chem. Soc.* 138:7733–40
53. Kocabey S, Kempter S, List J, Xing Y, Bae W, et al. 2015. Membrane-assisted growth of DNA origami nanostructure arrays. *ACS Nano* 9:3530–39
54. Aghebat Rafat A, Pirzer T, Scheible MB, Kostina A, Simmel FC. 2014. Surface-assisted large-scale ordering of DNA origami tiles. *Angew. Chem. Int. Ed. Engl.* 53:7665–68
55. Suzuki Y, Endo M, Sugiyama H. 2015. Lipid-bilayer-assisted two-dimensional self-assembly of DNA origami nanostructures. *Nat. Commun.* 6:8052
56. Woo S, Rothemund PWK. 2014. Self-assembly of two-dimensional DNA origami lattices using cation-controlled surface diffusion. *Nat. Commun.* 5:4889
57. Douglas SM, Marblestone AH, Teerapittayanon S, Vazquez A, Church GM, Shih WM. 2009. Rapid prototyping of 3D DNA-origami shapes with caDNAno. *Nudeic Acids Res.* 37:5001–6
58. Castro CE, Su HJ, Marras AE, Zhou L, Johnson J. 2015. Mechanical design of DNA nanostructures. *Nanoscale* 7:5913–21
59. Bustamante C, Marko JF, Siggia ED, Smith S. 1994. Entropic elasticity of lambda-phage DNA. *Science* 265:1599–600
60. Wang MD, Yin H, Landick R, Gelles J, Block SM. 1997. Stretching DNA with optical tweezers. *Biophys. J.* 72:1335–46
61. Pan J, Li F, Cha TG, Chen H, Choi JH. 2015. Recent progress on DNA based walkers. *Curr. Opin. Biotechnol.* 34:56–64
62. Sherman WB, Seeman NC. 2004. A precisely controlled DNA biped walking device. *Nano Lett.* 4:1203–7
63. Shin JS, Pierce NA. 2004. A synthetic DNA walker for molecular transport. *J. Am. Chem. Soc.* 126:10834–35
64. Omabegho T, Sha R, Seeman NC. 2009. A bipedal DNA Brownian motor with coordinated legs. *Science* 324:67–71
65. Green SJ, Bath J, Turberfield AJ. 2008. Coordinated chemomechanical cycles: a mechanism for autonomous molecular motion. *Phys. Rev. Lett.* 101:238101
66. Jung C, Allen PB, Ellington AD. 2016. A stochastic DNA walker that traverses a microparticle surface. *Nat. Nanotechnol.* 11:157–63
67. Yin P, Choi HM, Calvert CR, Pierce NA. 2008. Programming biomolecular self-assembly pathways. *Nature* 451:318–22
68. Bath J, Green SJ, Turberfield AJ. 2005. A free-running DNA motor powered by a nicking enzyme. *Angew. Chem. Int. Ed. Engl.* 44:4358–61
69. Bath J, Green SJ, Allen K, Turberfield AJ. 2009. Mechanism for a directional, processive, and reversible DNA motor. *Small* 5:1513–16
70. Cha TG, Pan J, Chen H, Salgado J, Li X, et al. 2014. A synthetic DNA motor that transports nanoparticles along carbon nanotubes. *Nat. Nanotechnol.* 9:39–43
71. Zhou C, Duan X, Liu N. 2015. A plasmonic nanorod that walks on DNA origami. *Nat. Commun.* 6:8102
72. Yehl K, Mugler A, Vivek S, Liu Y, Zhang Y, et al. 2016. High-speed DNA-based rolling motors powered by RNase H. *Nat. Nanotechnol.* 11:184–90
73. Zhang Z, Olsen EM, Kryger M, Voigt NV, Torring T, et al. 2011. A DNA tile actuator with eleven discrete states. *Angew. Chem. Int. Ed. Engl.* 50:3983–87
74. Ranallo S, Prévost-Tremblay C, Idili A, Vallée-Bélisle A, Ricci F. 2017. Antibody-powered nucleic acid release using a DNA-based nanomachine. *Nat. Commun.* 8:15150
75. Gu H, Yang W, Seeman NC. 2010. DNA scissors device used to measure MutS binding to DNA mis-pairs. *J. Am. Chem. Soc.* 132:4352–57
76. Modi S, Nizak C, Surana S, Halder S, Krishnan Y. 2013. Two DNA nanomachines map pH changes along intersecting endocytic pathways inside the same cell. *Nat. Nanotechnol.* 8:459–67

77. Chatterjee G, Dalchau N, Muscat RA, Phillips A, Seelig G. 2017. A spatially localized architecture for fast and modular DNA computing. *Nat. Nanotechnol.* 12:920–27
78. Kopperger E, Pirzer T, Simmel FC. 2015. Diffusive transport of molecular cargo tethered to a DNA origami platform. *Nano Lett.* 15:2693–99
79. Zhang F, Nangreave J, Liu Y, Yan H. 2012. Reconfigurable DNA origami to generate quasifractal patterns. *Nano Lett.* 12:3290–95
80. Song J, Li Z, Wang P, Meyer T, Mao C, Ke Y. 2017. Reconfiguration of DNA molecular arrays driven by information relay. *Science* 357:eaan3377
81. Zadegan RM, Jepsen MD, Thomsen KE, Okholm AH, Schaffert DH, et al. 2012. Construction of a 4 zeptoliters switchable 3D DNA box origami. *ACS Nano* 6:10050–53
82. Banerjee A, Bhatia D, Saminathan A, Chakraborty S, Kar S, Krishnan Y. 2013. Controlled release of encapsulated cargo from a DNA icosahedron using a chemical trigger. *Angew. Chem. Int. Ed. Engl.* 52:6854–57
83. Kohman RE, Han X. 2015. Light sensitization of DNA nanostructures via incorporation of photocleavable spacers. *Chem. Commun.* 51:5747–50
84. Kuzyk A, Schreiber R, Zhang H, Govorov AO, Liedl T, Liu N. 2014. Reconfigurable 3D plasmonic metamolecules. *Nat. Mater.* 13:862–66
85. Sobczak JP, Martin TG, Gerling T, Dietz H. 2012. Rapid folding of DNA into nanoscale shapes at constant temperature. *Science* 338:1458–61
86. Ketterer P, Willner EM, Dietz H. 2016. Nanoscale rotary apparatus formed from tight-fitting 3D DNA components. *Sci. Adv.* 2:e1501209
87. Marras AE, Zhou L, Su HJ, Castro CE. 2015. Programmable motion of DNA origami mechanisms. *PNAS* 112:713–18
88. Ke Y, Meyer T, Shih WM, Bellot G. 2016. Regulation at a distance of biomolecular interactions using a DNA origami nanoactuator. *Nat. Commun.* 7:10935
89. Zhou L, Marras AE, Su HJ, Castro CE. 2015. Direct design of an energy landscape with bistable DNA origami mechanisms. *Nano Lett.* 15:1815–21
90. Gu H, Chao J, Xiao SJ, Seeman NC. 2010. A proximity-based programmable DNA nanoscale assembly line. *Nature* 465:202–5
91. Yin P, Yan H, Daniell XG, Turberfield AJ, Reif JH. 2004. A unidirectional DNA walker that moves autonomously along a track. *Angew. Chem. Int. Ed. Engl.* 43:4906–11
92. Lund K, Manzo AJ, Dabby N, Michelotti N, Johnson-Buck A, et al. 2010. Molecular robots guided by prescriptive landscapes. *Nature* 465:206–10
93. Pan J, Cha TG, Li F, Chen H, Bragg NA, Choi JH. 2017. Visible/near-infrared subdiffraction imaging reveals the stochastic nature of DNA walkers. *Sci. Adv.* 3:e1601600
94. Li N, Zheng J, Li C, Wang X, Ji X, He Z. 2017. An enzyme-free DNA walker that moves on the surface of functionalized magnetic microparticles and its biosensing analysis. *Chem. Commun.* 53:8486–88
95. Jung C, Allen PB, Ellington AD. 2017. A simple, cleated DNA walker that hangs on to surfaces. *ACS Nano* 11:8047–54
96. Wickham SF, Endo M, Katsuda Y, Hidaka K, Bath J, et al. 2011. Direct observation of stepwise movement of a synthetic molecular transporter. *Nat. Nanotechnol.* 6:166–69
97. Yang Y, Goetzfried MA, Hidaka K, You M, Tan W, et al. 2015. Direct visualization of walking motions of photocontrolled nanomachine on the DNA nanostructure. *Nano Lett.* 15:6672–76
98. Schnitzer MJ, Block SM. 1997. Kinesin hydrolyses one ATP per 8-nm step. *Nature* 388:386–90
99. Wang C, Tao Y, Song G, Ren J, Qu X. 2012. Speeding up a bidirectional DNA walking device. *Langmuir* 28:14829–37
100. Saha S, Prakash V, Halder S, Chakraborty K, Krishnan Y. 2015. A pH-independent DNA nanodevice for quantifying chloride transport in organelles of living cells. *Nat. Nanotechnol.* 10:645–51
101. Surana S, Bhat JM, Koushika SP, Krishnan Y. 2011. An autonomous DNA nanomachine maps spatiotemporal pH changes in a multicellular living organism. *Nat. Commun.* 2:340
102. Surana S, Shenoy AR, Krishnan Y. 2015. Designing DNA nanodevices for compatibility with the immune system of higher organisms. *Nat. Nanotechnol.* 10:741–47

103. Peng P, Shi L, Wang H, Li T. 2017. A DNA nanoswitch-controlled reversible nanosensor. *Nudeic Acids Res.* 45:541–46
104. Wei B, Ong LL, Chen J, Jaffe AS, Yin P. 2014. Complex reconfiguration of DNA nanostructures. *Angew. Chem. Int. Ed. Engl.* 53:7475–79
105. Hao Y, Kristiansen M, Sha R, Birktoft JJ, Hernandez C, et al. 2017. A device that operates within a self-assembled 3D DNA crystal. *Nat. Chem.* 9:824–27
106. Andersen ES, Dong M, Nielsen MM, Jahn K, Subramani R, et al. 2009. Self-assembly of a nanoscale DNA box with a controllable lid. *Nature* 459:73–76
107. Perrault SD, Shih WM. 2014. Virus-inspired membrane encapsulation of DNA nanostructures to achieve in vivo stability. *ACS Nano* 8:5132–40
108. Ponnuswamy N, Bastings MMC, Nathwani B, Ryu JH, Chou LYT, et al. 2017. Oligolysine-based coating protects DNA nanostructures from low-salt denaturation and nuclease degradation. *Nat. Commun.* 8:15654
109. Lee H, Lytton-Jean AK, Chen Y, Love KT, Park AI, et al. 2012. Molecularly self-assembled nucleic acid nanoparticles for targeted in vivo siRNA delivery. *Nat. Nanotechnol.* 7:389–93
110. Zhang Q, Jiang Q, Li N, Dai L, Liu Q, et al. 2014. DNA origami as an in vivo drug delivery vehicle for cancer therapy. *ACS Nano* 8:6633–43
111. Funke JJ, Dietz H. 2016. Placing molecules with Bohr radius resolution using DNA origami. *Nat. Nanotechnol.* 11:47–52
112. Marras AE, Zhou L, Kolliopoulos V, Su HJ, Castro CE. 2016. Directing folding pathways for multicomponent DNA origami nanostructures with complex topology. *New J. Phys.* 18:055005
113. Gerling T, Wagenbauer KF, Neuner AM, Dietz H. 2015. Dynamic DNA devices and assemblies formed by shape-complementary, non–base pairing 3D components. *Science* 347:1446–52
114. Zhou L, Marras AE, Su HJ, Castro CE. 2013. DNA origami compliant nanostructures with tunable mechanical properties. *ACS Nano* 8:27–34
115. Zhou L, Marras AE, Castro CE, Su H-J. 2016. Pseudorigid-body models of compliant DNA origami mechanisms. *J. Mech. Robot.* 8:051013
116. Liedl T, Högberg B, Tytell J, Ingber DE, Shih WM. 2010. Self-assembly of three-dimensional prestressed tensegrity structures from DNA. *Nat. Nanotechnol.* 5:520–24
117. Shi Z, Castro CE, Arya G. 2017. Conformational dynamics of mechanically compliant DNA nanostructures from coarse-grained molecular dynamics simulations. *ACS Nano* 11:4617–30
118. Yurke B, Turberfield AJ, Mills AP Jr., Simmel FC, Neumann JL. 2000. A DNA-fuelled molecular machine made of DNA. *Nat* 406:605–8
119. Liu M, Fu J, Hejesen C, Yang Y, Woodbury NW, et al. 2013. A DNA tweezer–actuated enzyme nanoreactor. *Nat. Commun.* 4:2127
120. Kuzyk A, Urban MJ, Idili A, Ricci F, Liu N. 2017. Selective control of reconfigurable chiral plasmonic metamolecules. *Sci. Adv.* 3:e1602803
121. Yang Y, Endo M, Hidaka K, Sugiyama H. 2012. Photo-controllable DNA origami nanostructures assembling into predesigned multiorientational patterns. *J. Am. Chem. Soc.* 134:20645–53
122. Hudoba MW, Luo Y, Zacharias A, Poirier MG, Castro CE. 2017. Dynamic DNA origami device for measuring compressive depletion forces. *ACS Nano* 11:6566–73
123. Zhang DY, Seelig G. 2011. Dynamic DNA nanotechnology using strand-displacement reactions. *Nat. Chem.* 3:103–13
124. Srinivas N, Ouldridge TE, Sulc P, Schaeffer JM, Yurke B, et al. 2013. On the biophysics and kinetics of toehold-mediated DNA strand displacement. *Nudeic Acids Res.* 41:10641–58
125. Kuzyk A, Yang Y, Duan X, Stoll S, Govorov AO, et al. 2016. A light-driven three-dimensional plasmonic nanosystem that translates molecular motion into reversible chiroptical function. *Nat. Commun.* 7:10591
126. Yang Y, Tashiro R, Suzuki Y, Emura T, Hidaka K, et al. 2017. A photoregulated DNA-based rotary system and direct observation of its rotational movement. *Chemistry* 23:3979–85
127. Asanuma H, Liang X, Nishioka H, Matsunaga D, Liu M, Komiyama M. 2007. Synthesis of azobenzene-tethered DNA for reversible photo-regulation of DNA functions: hybridization and transcription. *Nat. Protoc.* 2:203–12

128. List J, Weber M, Simmel FC. 2014. Hydrophobic actuation of a DNA origami bilayer structure. *Angew. Chem. Int. Ed. Engl.* 53:4236–39
129. Mukherjea M, Llinas P, Kim H, Travaglia M, Safer D, et al. 2009. Myosin VI dimerization triggers an unfolding of a three-helix bundle in order to extend its reach. *Mol. Cell* 35:305–15
130. Yildiz A, Tomishige M, Gennerich A, Vale RD. 2008. Intramolecular strain coordinates kinesin stepping behavior along microtubules. *Cell* 134:1030–41
131. Kinosita K Jr., Yasuda R, Noji H, Adachi K. 2000. A rotary molecular motor that can work at near 100% efficiency. *Philos. Trans. R. Soc. B* 355:473–89
132. List J, Falgenhauer E, Kopperger E, Pardatscher G, Simmel FC. 2016. Long-range movement of large mechanically interlocked DNA nanostructures. *Nat. Commun.* 7:12414
133. Sun L, Zhang X, Gao S, Rao PA, Padilla-Sanchez V, et al. 2015. Cryo-EM structure of the bacteriophage T4 portal protein assembly at near-atomic resolution. *Nat. Commun.* 6:7548
134. Gligoris T, Lowe J. 2016. Structural insights into ring formation of cohesin and related Smc complexes. *Trends Cell Biol.* 26:680–93
135. Corbett KD, Harrison SC. 2016. Molecular architecture of the yeast monopolin complex. *Cell Rep.* 17:929
136. Le JV, Luo Y, Darcy MA, Lucas CR, Goodwin MF, et al. 2016. Probing nucleosome stability with a DNA origami nanocaliper. *ACS Nano* 10:7073–84
137. Funke JJ, Ketterer P, Lieleg C, Schunter S, Korber P, Dietz H. 2016. Uncovering the forces between nucleosomes using DNA origami. *Sci. Adv.* 2:e1600974
138. Chen Y-J, Groves B, Muscat RA, Seelig G. 2015. DNA nanotechnology from the test tube to the cell. *Nat. Nanotechnol.* 10:748–60
139. Groves B, Chen YJ, Zurla C, Pochekailov S, Kirschman JL, et al. 2016. Computing in mammalian cells with nucleic acid strand exchange. *Nat. Nanotechnol.* 11:287–94
140. Wang K, Tang Z, Yang CJ, Kim Y, Fang X, et al. 2009. Molecular engineering of DNA: molecular beacons. *Angew. Chem. Int. Ed. Engl.* 48:856–70
141. Li D, Song S, Fan C. 2010. Target-responsive structural switching for nucleic acid–based sensors. *Acc. Chem. Res.* 43:631–41
142. Bell NA, Engst CR, Ablay M, Divitini G, Ducati C, et al. 2012. DNA origami nanopores. *Nano Lett.* 12:512–17
143. Endo M, Sugiyama H. 2014. Single-molecule imaging of dynamic motions of biomolecules in DNA origami nanostructures using high-speed atomic force microscopy. *Acc. Chem. Res.* 47:1645–53
144. Ke Y, Lindsay S, Chang Y, Liu Y, Yan H. 2008. Self-assembled water-soluble nucleic acid probe tiles for label-free RNA hybridization assays. *Science* 319:180–83
145. Kuzuya A, Sakai Y, Yamazaki T, Xu Y, Komiyama M. 2011. Nanomechanical DNA origami "single-molecule beacons" directly imaged by atomic force microscopy. *Nat. Commun.* 2:449
146. Walter HK, Bauer J, Steinmeyer J, Kuzuya A, Niemeyer CM, Wagenknecht HA. 2017. "DNA origami traffic lights" with a split aptamer sensor for a bicolor fluorescence readout. *Nano Lett.* 17:2467–72
147. Liu M, Fu J, Hejesen C, Yang Y, Woodbury NW, et al. 2013. A DNA tweezer–actuated enzyme nanoreactor. *Nat. Commun.* 4:2127
148. Jungmann R, Steinhauer C, Scheible M, Kuzyk A, Tinnefeld P, Simmel FC. 2010. Single-molecule kinetics and super-resolution microscopy by fluorescence imaging of transient binding on DNA origami. *Nano Lett.* 10:4756–61
149. Jungmann R, Avendano MS, Dai MJ, Woehrstein JB, Agasti SS, et al. 2016. Quantitative super-resolution imaging with qPAINT. *Nat. Methods* 13:439–42
150. Bhatia D, Arumugam S, Nasilowski M, Joshi H, Wunder C, et al. 2016. Quantum dot–loaded monofunctionalized DNA icosahedra for single-particle tracking of endocytic pathways. *Nat. Nanotechnol.* 11:1112–19
151. Jiang Q, Song C, Nangreave J, Liu X, Lin L, et al. 2012. DNA origami as a carrier for circumvention of drug resistance. *J. Am. Chem. Soc.* 134:13396–403
152. Zhao Y-X, Shaw A, Zeng X, Benson E, Nyström AM, Högberg B. 2012. DNA origami delivery system for cancer therapy with tunable release properties. *ACS Nano* 6:8684–91

153. Zhang Q, Jiang Q, Li N, Dai L, Liu Q, et al. 2014. DNA origami as an in vivo drug delivery vehicle for cancer therapy. *ACS Nano* 8:6633–43
154. Schüller VJ, Heidegger S, Sandholzer N, Nickels PC, Suhartha NA, et al. 2011. Cellular immunostimulation by CpG-sequence-coated DNA origami structures. *ACS Nano* 5:9696–702
155. Kohman RE, Cha SS, Man HY, Han X. 2016. Light-triggered release of bioactive molecules from DNA nanostructures. *Nano Lett.* 16:2781–85
156. Li F, Chen H, Pan J, Cha TG, Medintz IL, Choi JH. 2016. A DNAzyme-mediated logic gate for programming molecular capture and release on DNA origami. *Chem. Commun.* 52:8369–72

Annual Review
of Biomedical
Engineering

Volume 20, 2018

Contents

Errata

An online log of corrections to *Annual Review of Biomedical Engineering* articles may be found at http://www.annualreviews.org/errata/bioeng